Poole, A., Wersall, A., Brown, E., & Williams, C. (2018). Mouse platelet Ral GTPases control P-selectin surface expression, regulating platelet-leukocyte interaction: Ral GTPases control P-selectin surface expression. Arteriosclerosis, Thrombosis, and Vascular Biology.

Mouse platelet Ral GTPases control P-selectin surface expression, regulating platelet-leukocyte interaction.

Authors: Andreas Wersäll[1*], Chris M. Williams[1], Edward Brown[1], Tommaso Iannitti[2], Neil Williams[2] and Alastair W. Poole[1]

Affiliations:
[1]School of Physiology, Pharmacology & Neuroscience, University of Bristol, Bristol, BS8 1TD, UK.
[2]KWS Biotest, Marine View Office Park, 47-48 Martingale Way, Portishead, Bristol, BS20 7AW, UK.

Running title: Ral GTPases control P-selectin surface expression

Keywords: Platelets, Cell Signaling/Signal Transduction, Inflammation

Word count: 4552 (main text)

Total number of figures & tables: 6 (+8 supplemental)

TOC Category: Basic

TOC Subcategory: Thrombosis

Abstract

Objective: RalA and RalB GTPases are important regulators of cell growth, cancer metastasis and granule secretion. The purpose of this study was to determine the role of Ral GTPases in platelets with the use of platelet specific gene-knockout (KO) mouse models.

Approach and Results: This study shows that platelets from double knockout mice (DKO), in which both GTPases have been deleted, show markedly diminished (approx. 85 % reduction) P-selectin translocation to the surface membrane, suggesting a critical role in α-granule secretion. Surprisingly however there were only minor effects on stimulated release of soluble α- and δ-granule content, with no alteration in granule count, morphology or content. In addition, their expression was not essential for platelet aggregation or thrombus formation. However, absence of surface P-selectin caused a marked reduction (approx. 70 %) in platelet-leukocyte interactions in blood from RalAB DKO mice, suggesting a role for platelet Rals in platelet-mediated inflammation.

Conclusions: Platelet Ral GTPases primarily control P-selectin surface expression, in turn regulating platelet-leukocyte interaction. Ral GTPases could therefore be important novel targets for the selective control of platelet-mediated immune cell recruitment and inflammatory disease.

Nonstandard Abbreviations and Acronyms

α-granule	Alpha granule
δ-granule	Dense granule
CRP-XL	Cross linked collagen related peptide
PAR4-AP	Protease-activated receptor 4-activating peptide
PF4	Platelet factor 4
TGF-β	Transforming growth factor beta

Introduction

Ral GTPases, RalA and RalB, are Ras-like small GTPases that are important mediators of tumour growth and metastasis, with Ral inhibitor compounds currently being developed as novel anti-cancer agents[1-3]. In addition, they have key roles to play in membrane trafficking and secretion via interactions with their effector, the exocyst complex[4,5]. Widely expressed in human tissues, the exocyst is an octameric protein complex involved in tethering secretory vesicles to plasma membranes, preceding N-ethylmaleimide–sensitive factor attachment protein receptor (SNARE) complex formation and exocytosis[5,6]. In platelets, regulatory GTPases such as Rab27b, RhoA/G and Rap1b all play major roles in platelet function, acting as molecular switches in signalling pathways, themselves being regulated by guanine exchange factors (GEFs) and GTPase activating proteins (GAPs)[7-9]. Rals have been shown to be expressed in platelets, but are yet to be extensively investigated in these cells.

Platelet activation at sites of vascular damage leads to the release of over 300 bioactive molecules from distinct secretory granules[10,11]. Dense (δ) granules predominantly contain small molecules with platelet-activating properties, aiding recruitment of platelets to a growing thrombus[12]. The contents and roles of alpha (α) granules are more varied, with studies highlighting roles for α-granule releasates in immune responses and wound healing, as well as angiogenesis and tumour metastasis[13]. Importantly, α-granules also express cell adhesion molecules such as P-selectin on their membranes which translocate to the platelet membrane upon granule fusion, mediating interaction with leukocytes - regulating their extravasation into tissues[14,15]. As the functions associated with platelet releasates are so varied, platelet secretion is a tightly regulated process[16,17].

Little is known about the role of platelet Ral GTPases. Previous studies have shown that both RalA/B become activated upon platelet stimulation in a Ca^{2+}-dependent manner, and the use of functional blocking antibodies in a permeabilised platelet system highlighted roles for Rals in δ-granule secretion via exocyst interactions[18,19]. However, due to a lack of knockout models and the limitations associated with the use of permeabilised platelet systems, elucidating fully the roles of platelet Rals has not previously been possible.

In this study we have generated the first murine platelet-specific knockouts for RalA, RalB and both together (RalAB), to definitively investigate the roles of these GTPases in platelets. Results show that the presence of at least one Ral isoform is necessary for P-selectin expression on the platelet membrane, with RalAB double knockout (DKO) platelets showing an 85% reduction in P-selectin expression in response to platelet stimulation. Surprisingly however, release of α-granule cargo is largely unaltered in the RalAB DKO, pointing to the possibility that Ral GTPases do not control all aspects of α-granule secretion. Furthermore, δ-granule secretion was only marginally reduced in the RalAB DKO, with no significant effect observed in aggregation or thrombus formation assays. The markedly diminished P-selectin exposure in the absence of RalAB leads to a substantial reduction in platelet-leukocyte interactions. The $Pf4\text{-}Cre^{+}$ $RalA/B^{flox}$ mice also show a delay in the onset of dextran sulfate sodium (DSS)-induced ulcerative colitis symptoms *in vivo*. Taken together these results suggest that platelet Rals may contribute to platelet-mediated immune responses and targeting them may provide a

novel and selective approach to the treatment of certain inflammatory diseases, while also providing caution regarding the use of Ral inhibitors in the treatment of cancer[2].

Materials & Methods

Materials - RalA and RalB rabbit monoclonal antibodies were from Cell Signalling Technology (Beverly, USA) supplied by NEB (New England Biolabs) (Hitchin, UK) [#3526 and #3523]. RalA mouse monoclonal antibody was from BD (Becton Dickson) Biosciences (Oxford, UK) [#610222]. EXOC2/Sec5 antibody was from Protein Technologies (Manchester, UK) [#12751-1-AP]. EXOC3/Sec6 antibody was from EMD Millipore (Billerica, USA) [#559240]. EXOC4/Sec8 antibody was from Abcam (Cambridge, UK) [#ab13254]. FITC-conjugated GPVI [#M011-1], GP1b [#M040-1], Integrin α_2 [#M071-1], P-selectin/CD62P [#M130-1] and PE-conjugated JON/A anti-integrin $\alpha_{IIb}\beta_3$ [#M023-2] were from Emfret Analytics (Eibelstadt, Germany). FITC-conjugated CD41 antibody was from Bio-Rad (Hemel Hempstead, UK) [#MCA2245F] with the PE-conjugated CD45 antibody supplied by BioLegend (London, UK) [#30-F11]. P-selectin and vWf antibodies were from Santa Cruz bioscience (Texas, USA) [#SC-6943 and #H-300] alongside control cell lysates for PC-12 [#SC-2250], NRK [#SC-364199] and RPE-1 [#SC-24771]. ActinGreen F-actin probe was from Life Technologies (Warrington, UK) [#R37110]. OneComp eBeads were from eBioscience (Hatfield, UK) [01-1111-42]. CRP-XL (collagen related peptide) was provided by Professor Richard Ferndale (University of Cambridge, UK). Chrono-lume ATP detection kit was from Labmedics (Manchester, UK) [#P/N 395]. GST (glutathione sepharose transferase) beads were from GE healthcare (Little Chalfont, UK) [#17075601], with the GST-RalBP1 (Ral binding protein 1)/RLIP76 construct being generously gifted by Ingrid Verlaan-Klink (Utrecht University, Netherlands). RalA Q75L [#19719], RalA S31N [#19718], RalB Q72L [#19721], RalB S28N [#19722] constructs[1] were supplied by Addgene (Cambridge, USA). NuPAGE LDS Sample buffer was from Life Technologies (Warrington, UK) [#NP0008]. Western blotting equipment was from Bio-Rad (Hemel Hempstead, UK) [#1703930] with ECL (enhanced chemiluminescent) detection reagents from GE healthcare (Little Chalfont, UK) [#RPN2232] and PVDF (polyvinylidene difluoride) transfer membrane (Immobilon P/FL) from Millipore (Nottingham, UK) [#IPVH00010]. Ibidi slides [#80661] and elbow luers [#10802] were from Thistle Scientific (Glasgow, UK). Horm fibrillary collagen was from Takeda Pharma (Linz, Austria) [#1128818]. Ketamine was from Pfizer (Kent, UK) [#EN-3179]. Xylazine was from Bayer (Reading, UK) [#1040032]. DyLight 488-conjugated anti-GPIbβ antibody was from Novus Biologicals (Abingdon, UK) [#NB100-63790G]. 5 mL round-bottom polystyrene FACS tubes were supplied by BD Biosciences (Oxford, UK) [#352235]. Red blood cell lysis (RBC) buffer was from Roche (Basel, Switzerland) [#11814389001]. Mouse TGF-β [#DY1679] and PF4 ELISA kits [#DY595], as well as angiogenesis microarray kits [#ARY015] were from R&D Systems (Abingdon, UK). ProLong Diamond Antifade mountant was from Life Technologies (Warrington, UK) [#P36965]. Dextran sulfate sodium (DSS) was provided by KWS Biotest (Portishead, UK). All agonist preparations were made up in modified HEPES-Tyrode's unless otherwise stated, with unlisted reagents all supplied by Sigma Aldrich (Dorset, UK).
Mice - A colony of $RalA^{flox/flox}$ and $RalB^{flox/flox}$ mice were generously provided by Professor Chris Marshall, Institute of Cancer Research, London[20]. Mice were crossed with Cre-PF4 mice to create $RalA^{flox/flox}$:Cre^{+} (RalA KO), $RalA^{flox/flox}$:Cre^{-} (RalA WT [Wild-type]), $RalB^{flox/flox}$:Cre^{+} (RalB KO) and $RalB^{flox/flox}$:Cre^{-} (RalB WT) mice. Subsequently,

RalA$^{flox/flox}$:Cre^{+} mice were crossed with RalB$^{flox/flox}$:Cre^{-} mice to generate RalA$^{flox/flox}$:RalB$^{flox/flox}$:Cre^{+} (RalAB DKO) and RalA$^{flox/flox}$:RalB$^{flox/flox}$:Cre^{-} (RalAB WT). 8-24 week age and sex matched mice were used in all experiments, with data from male and female mice analysed and presented together. The local ethics committee at the University of Bristol, UK, approved all animal studies and mice were bred for this purpose under the UK Home Office project license PPL30/2908.

Human and mouse platelet preparation – Human blood was obtained from healthy volunteers in accordance with the local research ethics committee at the University of Bristol (LREC number E5736). Animals were sacrificed by CO_2 asphyxiation and blood was drawn from the inferior (caudal) vena cava as previously described[21]. Platelets were prepared as previously described[22] and rested for 30 min at 30°C in the presence of 10 μM indomethacin and 0.02 units/ml of apyrase prior to stimulation. For flow cytometry and releasate studies, washed mouse platelets were recalcified to a final concentration of 1 mM with $CaCl_2$ 1 minute prior to stimulation.

Generation of GST fusion proteins – pGEX4T1-GST-RalBP1 and Ral mutant constructs were generated as previously described[18]. Ral mutants were PCR cloned into a pGEX4T1 vector before generation of GST-beads using standard techniques. Briefly, BL21(DE3)pLysS protease-negative bacteria from Agilent Technologies (Cheadle, UK) were transformed and grown to log phase in 500 mL of LB (lysogeny broth) media supplemented with 0.5 % glucose before induction with 0.2 mM IPTG (isopropyl β-D-1-thiogalactopyranoside) for 3 h at 30 ^{o}C. Bacteria were pelleted by centrifugation before resuspension in 15 mL of PBS lysis solution (1 x PBS, 1 mM DTT [Dithiothreitol], 1 x complete protease tablet/50 mL, 0.1 % Triton-X) and sonicated. Bacterial lysate was then centrifuged at 27,000 *g* and supernatant collected, before incubation with GST beads for 1 hr on a roller.

Pulldown assays – 300 μl of human platelets at 4 x 10^8 platelets/ml were stimulated with indicated agonists before lysis with 2x NP40 buffer (20 % glycerol, 2 % NP40, 400 mM NaCl, 50 mM HEPES, 5 mM $MgCl_2$, 2 μM microcystin-LR, 1 x complete mini EDTA-free protease inhibitor tablet/5 mL). Lysates were placed on ice for 10 min with 30 μl removed and added to 4 x LDS sample buffer supplemented with 50 mM DTT to be used as a loading control. Remaining lysate was clarified by centrifugation before rotation for 1 h at 4 ^{o}C with 25 μl of GST-bead slurry. Beads were washed with ice-cold 1 x NP40 buffer three times before addition of 20 μl 2 x LDS sample buffer with DTT. Input and pull-down samples were incubated at 80 ^{o}C for 10 min before analysis by immunoblotting.

Electrophoresis and immunoblotting - Appropriate percentage tris-glycine SDS (sodium dodecyl sulphate)-polyacrylamide gels were used to run platelet proteins. Gels were then transferred onto either Immobilon P or FL depending on the developer in use (P for an ECL system, FL for a fluorescence system). Membranes were blocked for an hour at RT in 5 % BSA (bovine serum albumin) before subsequent incubation with primary and secondary antibodies between several wash stages. Proteins were either detected using an ECL and film detection system or a fluorescence based Li-Cor

Odyssey CLx (Lincoln, USA).

Quantification of integrin $\alpha_{IIb}\beta_3$ activation and P-selectin expression – Flow cytometry analysis of platelets was performed as previously described[23]. Samples were analysed on a BD Biosciences FACScan flow cytometer, with raw data exported and analysed using Flowing Software.

Quantification of PF4 and TGF-β secretion – Washed mouse platelets at 2 x 10^8 platelets/mL were stimulated with indicated concentrations of agonist for designated time periods at 37 ^oC, before centrifugation at 650 *g* for 1 min to isolate releasate. Control total samples were generated by lysing unstimulated platelets with an equal volume of 1 % Triton-X before 3 cycles of snap freezing. For PF4 studies releasate and total samples were diluted 1/250 and 1/500 in reagent diluent (0.5 % BSA, 0.05 % TWEEN in PBS). In TGF-β studies releasate and total samples were diluted 1/20 and 1/40 respectively. Determination of PF4 and TGF-β levels were achieved with the use of appropriate kits, where concentration of analytes was achieved with the generation of a standard curve. All kits were used according to the manufacturer's protocol, with colorimetric readout at 450/540nm achieved with the use of a TECAN Infinite 200 PRO microplate reader (Reading, UK).

Antibody microarray analysis of platelet releasate – 800 µl aliquots of mouse platelets at 4 x 10^8 platelets/mL were stimulated with 3 µg/mL CRP-XL for 10 min at 37 ^oC, before centrifugation at 650 *g* for 10 min to isolate releasate. 700 µl of releasate was supplemented with 300 µl Array Buffer 6 and 500 µl Array Buffer 4 before completion of the assay according to manufacturer's instruction. Proteins were detected with an ECL and film system before quantification with ImageJ.

Immunofluorescence – Platelets were prepared as previously described with minor modifications[24]. Mouse PRP was fixed with 4 % PFA and 1 % BSA in PBS for 15 min before being spotted onto coverslips. Platelets were incubated in 100 % humidity at 37 ^oC for 90 min before rinsing with PBS and permeabilisation with 0.2 % Triton-X. Platelets were blocked with 0.2 % BSA for 30 min before immunostaining with designated antibodies or IgG controls overnight, with unstained and secondary-only samples also used as controls. Coverslips were mounted before images were acquired with a Leica SP5-AOBS confocal laser scanning microscope attached to a Leica SM I6000 inverted epifluorescence microscope. Deconvolution of images and post processing was achieved with the use of Huygens Professional and Volocity.

In vitro thrombus formation – Quantification of thrombus formation on collagen under flow was performed as previously described[25]. Briefly, IBIDI µ-Slide VI$^{0.1}$ chips were coated with 50 µg/mL collagen for 2 hr before being flushed and blocked with 2 % fatty acid free (FAF) BSA prepared in HEPES Tyrode's buffer. Mouse blood was taken as above and anticoagulated with 2000 U/ml heparin and 20 µM PPACK (1:9 v/v) before loading with 2 µM $DiOC_6$. Blood was then transferred to a 1 mL syringe and perfused using an Aladdin AL-1000 syringe pump (World precision instruments, UK) at a shear rate of 1000 s^{-1} for 2 min. Platelets were fixed by perfusion of 4 % PFA through

channels for 4 min before non-adherent cells were flushed away with HEPES Tyrode's buffer. IBIDI mounting medium was used to preserve fixed platelets for imaging. Thrombus formation was examined by generating confocal z-stacks (1024 x 1024 pixels, 0.5 µm stack distance) from 5 randomly chosen fields of view using a Leica SP5-II confocal laser scanning microscope attached to a Leica DMI 6000 inverted epifluorescence microscope (Leica Microsystems, UK).

Quantification of platelet aggregation and δ-granule secretion - Aggregometry and dense granule secretion assays were completed as previously described[22]. Aggregation results were expressed as "% Max Aggregation" and δ-granule secretion as "Peak ATP release in nM".

In vivo thrombus formation – Quantification of *in vivo* thrombus formation was performed as previously described[26]. Briefly, mice were anesthetized with 100 mg/kg ketamine and 10 mg/kg xylazine before labelling of platelets by intravenous administration of 100 mg/kg DyLight 488-conjugated anti-GPIbβ antibody (mice weighing over 30g were excluded from experiments). Carotid arteries were exposed before 15 % $FeCl_3$-soaked filter paper was placed on the arterial adventitia for 3 min. An Olympus BX51WI fixed stage microscope was used to acquire a time-lapse of the injury site for 20 min, with post processing of images completed with ImageJ. Background florescence values measured upstream of the injury site were subtracted from thrombus-specific fluorescence, and data are expressed as integrated density values.

Quantification of platelet-leukocyte aggregate formation – Mouse whole blood was anticoagulated with 4 % trisodium citrate and 2000 U/ml Heparin (1:10 v/v) before incubation with RBC lysis buffer (1:5.5 v/v) and agitated for 15 min before centrifugation at 500 *g* for 5 min. Half the volume of supernatant was aspirated and replaced with RBC lysis buffer before further agitation (10 min) and centrifugation. The formed pellet was resuspended in modified HEPES-Tyrode's solution to double the initial volume of whole blood, before stimulation with indicated concentrations of CRP-XL for 10 min. Samples were stained with 0.5 µg PE-CD45 and FITC-CD41 antibodies for 5 min before quenching by addition of HEPES-Tyrode's buffer (1:9 v/v). Samples were analysed by flow cytometry using a BD Biosciences Accuri C6 Sampler plus. Leukocyte populations were identified according to forward and side scatter profiles. Positive PE and FITC events within the leukocyte region signified platelet-leukocyte aggregates, with appropriate IgG antibody controls used to determine false positive results. Results are expressed as the median FITC signal present in the Pl-Leuk gate.

DSS-induced ulcerative colitis model – 10 8-10 week old RalAB WT and DKO mice littermate pairs were subject to a week of acclimatisation before their drinking water was replaced with a 5 % DSS solution. Over a 10-day period mice were given *ad libitum* access to the DSS solution while being monitored for clinical signs of colitis including bodyweight loss, loose stools and presence of occult or gross blood in stools. Clinical observations were given scores based on severity and subsequently graphed.

Transmission electron microscopy - Subcellular mouse platelet morphology was

analysed by transmission electron microscopy. Ultrathin counterstained sections were prepared as previously described[27]. ImageJ was then used to count dense and alpha granules in equivalent-sized fields of view.

Lysosomal secretion - Lysosomal secretion was determined using a β-hexosaminidase assay. Mouse platelets at 2 x 10^8 platelets/ml were stimulated with indicated concentrations of agonist for 10 min at 37 ^oC. Samples were then centrifuged at 650 *g* for 1 min to isolate releasates. Control total samples were generated by lysing unstimulated platelets with an equal volume of 1 % Triton-X before 3 cycles of snap freezing. 20 µl of releasate/control was then incubated with 20 µl of 5 mM P-NAG (4-Nitrophenyl N-acetyl-β-D-glucosaminide) made up in citrate phosphate buffer (80 mM Na_2HPO_4, 60 mM citric acid, pH 4.2) for 2 hr at 37 ^oC. Reactions were quenched with the addition of 200 µl of 0.1 M NaOH before reading of absorbance at 405 nm in an Opysys MR platereader made by Dynex Tehnologies (Worthing, UK)

Statistical analysis – All statistical analysis was performed with GraphPad Prism 5.03. All data are representative of >3 experiments, represented by mean ± standard error of the mean (exact number of repeats are detailed in figure legends). Antibody microarray data was n=2, with no statistical test performed (Supplementary Figure I). Normality testing was conducted with the use of a Kolmogorov-Smirnov test and supported by graphical inspection of data. T-tests and two-way ANOVA statistical tests were utilised where appropriate, with Bonferroni's post-hoc test used for two-way ANOVAs.

Results

Ral GTPases bind the exocyst upon platelet stimulation

Immunoblotting confirmed expression of the Ral GTPases in both human and murine platelets[28], with appropriate Ral deletion achieved in all gene-targeted Ral mouse lines (Figure 1A). Exocyst expression was confirmed by immunoblotting for components of the complex in platelet lysates alongside positive control lysates (Figure 1B)[29-31]. The data demonstrate the expression of the exocyst complex in both human and mouse platelets, supporting published platelet transcriptome studies[32].

Using a RalBP1-GST pulldown approach we showed that both RalA/B became maximally activated after 1 minute of stimulation with CRP-XL in human platelets (Figure 1C) – in line with previous findings[18]. Furthermore, we were able to show that Ral GTPases are activated by a panel of platelet agonists including ADP, U46619, CRP and PAR4-AP (Figure 1D).

To determine if activated Ral GTPases associate with the exocyst complex in platelets, constitutively active mutant forms of RalA (Q75L), RalB (Q72L) and their inactive counterparts (S31N and S28N)[1] were GST-tagged and used in a pulldown assay. Active forms of both RalA/B associated with Sec8/EXOC4 in basal and CRP stimulated conditions (Figure 1E), whereas there was no association of the exocyst with the inactive Ral mutants.

The presence of at least one Ral GTPase is essential for P-selectin expression on the surface membrane of mouse platelets

Flow cytometry was used to simultaneously measure P-selectin expression and integrin $\alpha_{IIb}\beta_3$ activation in mouse platelets. Stimulation of $RalA^{-/-}$ platelets with CRP-XL showed no difference between WT and KO (Figure 2A, D), whereas $RalB^{-/-}$ platelets showed a ~50 % reduction in P-selectin expression when stimulated with 10 µg/ml CRP-XL ($p < 0.01$), with no alteration to integrin $\alpha_{IIb}\beta_3$ activation (Figure 2B, E). Analysis of RalAB DKO platelets in these assays showed a ~85 % reduction in P-selectin expression at 3 ($p < 0.05$), 10 ($p < 0.001$) and 30 µg/ml CRP-XL ($p < 0.001$), with no change in integrin $\alpha_{IIb}\beta_3$ activation (Figure 2C, F).

Experiments were repeated with PAR4-AP to determine the agonist specificity of the effects seen for CRP-XL (Figure 2G, H), with DKO platelets showing a ~60 % reduction when compared with WT counterparts ($p < 0.001$). Samples were also prepared with the P_2Y_{12} blocker AR-C66096 (ARC, 10 µM) and stimulated with PAR4-AP to rule out any δ-granule secretion defects contributing to the defect in α-granule secretion, as previously described[33]. However, in the presence of ARC, the reduction in P-selectin expression in RalAB DKO mice is preserved, suggesting no contribution from δ-granule secretion. Importantly, integrin $\alpha_{IIb}\beta_3$ activation was not altered in response to PAR4-AP.

Ral deletion marginally alters α-granule cargo levels and release

The substantial reduction in stimulated P-selectin expression in RalAB DKO platelets suggested a major defect in α-granule secretion, so it was important to quantify α-

granule content and release in the RalAB WT and DKO platelets. PF4 and TGF-β release in response to platelet stimulation was assessed by ELISA (Figure 3A & B). The data however indicated no change in PF4 release, with only a small reduction in TGF-β release observed in response to 125 μM PAR4-AP ($p < 0.05$) – suggesting largely unaltered α-granule content release in DKO platelets. These data were further supported by the use of an antibody microarray to assess the effect of Ral deletion on a wider range of α-granule cargo, where relative levels of angiogenesis-associated polypeptides were determined in supernatants isolated from WT and DKO platelets stimulated with 3 μg/ml CRP-XL. Calculated DKO:WT ratios of the most abundant proteins present in samples from two separate assays showed no change in levels of released polypeptides between WT and DKO (Supplementary Figure I). Furthermore, lysosomal secretion as determined by measurement of released β-hexosaminidase was also unaltered in DKO platelets (Supplementary Figure II).

Due to the observed P-selectin defect, it was important to assess if P-selectin localisation was altered upon Ral deletion, which we determined by immunofluorescence microscopy (Figure 3C). Acquired images show P-selectin staining in the RalAB DKO is comparable to WT platelets, localising to granular compartments within the platelet.

Although the localisation of P-selectin was unaltered, it was also important to investigate expression levels of α-granule proteins within the RalAB WT and DKO platelets. Immunoblotting showed that P-selectin expression, normalised to loading control GAPDH, was marginally greater in RalAB DKO platelets compared to WT ($p < 0.05$, Figure 3D). Quantification of α-granule cargo content by ELISA showed no change in PF4 levels, but a marginally elevated level of TGF-β present within RalAB DKO platelets ($p < 0.05$, Figure 3D). Furthermore, TEM images of RalAB WT and DKO platelets showed no overt difference in morphology or granule numbers (Supplementary Figure IIIA, B). Taken together, these results indicate that Ral deletion does not cause major alterations in granule biogenesis or cargo loading.

Comparing kinetics of α-granule secretion highlights a major role for Ral GTPases in P-selectin surface expression

To gain further insight into the α-granule release reaction occurring in RalAB WT and DKO platelets we monitored levels of P-selectin surface expression, integrin $\alpha_{IIb}\beta_3$ activation, PF4 release and TGF-β release in response to stimulation with 3 μg/ml CRP-XL at pre-defined time points (Figure 4A, B, D, E). In addition, total platelet P-selectin levels upon stimulation were determined by western blotting to address whether P-selectin was lost in response to stimulation in transgenic mice (Figure 4C).

As determined by flow cytometry, we see an increasing difference in P-selectin surface exposure between the RalAB WT and DKO samples over time ($p < 0.001$), with a ~90 % reduction in P-selectin surface exposure observed in the RalAB DKO samples by 30 mins (Figure 4A). Measured simultaneously, we observed no change in integrin $\alpha_{IIb}\beta_3$ activation at the same time points (Figure 4B). These data are further supported by real-time monitoring of P-selectin exposure and integrin $\alpha_{IIb}\beta_3$ activation, again showing a

marked reduction in P-selectin exposure over 15 min in RalAB DKO platelets, but no change in integrin $\alpha_{IIb}\beta_3$ activation (Supplementary Figure IVA, B). Additionally, Ral deletion did not lead to an alteration in total P-selectin levels upon stimulation with 3 µg/ml CRP-XL or 125 µM PAR4-AP (Figure 4C).

Finally, measurement of PF4 and TGF-β release by ELISA over the same time points in response to 3 µg/ml CRP-XL highlighted no significant difference between RalAB WT and DKO (Figure 4D, E). Combined with data from Figure 3, these results indicate no major differences in soluble cargo release profiles of RalAB WT and DKO platelets, but a severe defect in P-selectin surface expression.

Ral deletion reduces δ-granule secretion in response to sub-maximal platelet stimuli, but does not affect aggregation or thrombus formation

Lumi-aggregometry was used to measure δ-granule secretion and platelet aggregation in response to platelet stimulation (Figure 5A, B). Deletion of RalA or RalB alone had no effect on δ-granule secretion or aggregation (Supplementary Figure V). RalAB DKO mice showed a small reduction in δ-granule secretion in response to 0.6 µg/ml CRP ($p < 0.01$) and 125 µM PAR-4 AP ($p < 0.05$), but this did not translate to a significant reduction in measured platelet aggregation.

Similarly, deletion of RalA or RalB did not alter thrombus formation *in vitro* (Supplementary Figure VI) and although thrombus volume and surface area were marginally reduced in the RalAB DKO platelets, this was not found to be significant (Figure 5C-E). Measurement of *in vivo* thrombus formation in a ferric chloride injury model again showed no change in the rate or extent of thrombus formation (Figure 5F-H). Furthermore, it is important to note that platelet Ral deletion has no effect on whole blood haematology values or platelet surface expression of CD41, GPVI, GPIb and integrin α_2 (Supplementary Figure IIIC, D), which could mask any alterations in aggregation and thrombus formation.

Platelet-leukocyte interactions are reduced in RalAB DKO mice when compared with WT

Platelet P-selectin is required for the initial tethering of activated platelets to leukocytes and endothelial cells[34,35]. This tethering allows leukocytes to be recruited to inflamed tissue through extravasation, which contributes to the development of pathologies such as inflammatory bowel disease (IBD) and rheumatoid arthritis[36,37]. As platelet Rals regulate stimulated P-selectin expression on the platelet membrane, it was possible that platelet-leukocyte interaction was disrupted for RalAB DKO platelets.

To determine if these interactions were altered, we measured platelet-leukocyte aggregate formation in response to platelet stimulation by CRP-XL (Figure 5). Whole blood from RalAB WT and DKO mice was subjected to RBC lysis before incubation with increasing concentrations of CRP-XL. Leukocytes and platelets were stained with CD45-PE and CD41-FITC before quenching of the reaction and subsequent analysis by flow cytometry. Appropriate IgG control samples were used to prevent measurement of false-positive events, allowing for generation of quadrant plots where single events

positive for both platelets (FITC) and leukocytes (PE) would be present in the top right quadrant – within the Pl-Leuk gate (Figure 5B). In Figure 5C, representative data from basal and CRP-stimulated WT/DKO mouse lines illustrates a reduced shift in FITC signal within the Pl-Leuk gate in the DKO sample upon stimulation, signifying platelets bound to leukocytes. Measurement of "Median FITC within Pl-Leuk" in all samples showed a ~70 % reduction in platelet-leukocyte interaction in the DKO mouse line, when compared with WT ($p < 0.001$), signifying fewer platelets bound to individual leukocytes in RalAB DKO samples (Figure 5D). Overall these results suggest that platelet Rals are critical for mediating this response, and may indicate a major role for these GTPases in inflammatory processes.

To further explore the role platelet Rals play in leukocyte extravasation and inflammatory conditions *in vivo*, RalAB WT and DKO mice were subject to a DSS-induced model of ulcerative colitis, where drinking water was replaced with 5 % DSS over a 10 day period as previously described[38,39]. The DSS model was chosen in particular due to previous studies highlighting the model's sensitivity to the presence of platelet mediated leukocyte extravasation, as well as P-selectin function[40-42].

Mice were monitored for symptoms associated with DSS-induced ulcerative colitis including bodyweight loss, stool consistency and presence of blood in stools, with scores generated based on severity (Supplementary Figure VIIA, B). An overall clinical score was generated by the addition of bodyweight and stool scores which was used as a measure of the progression of the DSS-induced ulcerative colitis model (Supplementary Figure VIIC). Results show a significant decrease in all measured parameters on day 4 of the study, with stool scores also significantly reduced on day 2. Taken together, these results suggest that at early stages of DSS-induced ulcerative colitis, platelet Ral deletion reduces the symptoms associated with the progression of the pathology. Although the study was carried out for 10 days, by day 8 over half the RalAB WT mice had to be culled due to reaching humane endpoints and for that reason data from the rest of the study is not shown. Upon termination, colons were dissected from mice and measured lengthways as a metric of gross pathology – revealing no significant alteration in terminal pathology (data not shown).

Discussion

Ral GTPases are important drivers of cell proliferation and metastasis in multiple human cancers, and as such are key targets for development of novel anti-cancer therapies. In addition, they have been shown to regulate cell adhesion and membrane trafficking including exocytosis, and so it was important to determine their contribution to platelet function. Here we showed that the two genes had overlapping and largely mutually redundant roles in regulating P-selectin externalisation, suggesting a role in regulating α-granule secretion. Surprisingly however dual Ral deletion had no overt effect upon release of α-granule content, whilst substantially blocking P-selectin surface expression. This has implications for the effects of Ral blockade on platelet function, which may specifically abrogate platelet-leukocyte interaction and subsequent inflammatory responses, without significantly affecting platelet function in thrombosis. This would allow the development of targeted therapies for diseases of platelet-mediated inflammation.

In the present study we showed the expression of RalA and RalB in both human and mouse platelets, generating the first genetically modified mouse lines with platelet-specific deletion of RalA, RalB and both together (Figure 1A). Previously published work showed that both RalA/B became maximally activated 1 min after platelet stimulation and were activated by numerous platelet agonists[18], and our data in Figure 1C&D are consistent with these findings. As one of the main effectors of Rals is the exocyst complex[4,5,43], we used GST-bound constitutively active and inactive forms of Ral GTPases to pull down interactors, and were able to confirm that active Ral GTPases bind the exocyst complex upon activation (Figure 1E). It is therefore likely that Rals mediate their activity in platelets through activation of the exocyst complex.

Quantification of P-selectin expression by flow cytometry revealed significant defects in both RalB KO and RalAB DKO platelets, suggesting Ral GTPases play key roles in α-granule secretion (Figure 2). The results also imply a degree of functional redundancy between the two GTPases, as the reduction in α-granule secretion observed in the RalAB DKO (~85 %) was greater than the sum of reduction in both RalA KO (0 %) and RalB KO (~50 %) mouse lines. Data also indicate that RalB is the dominant isoform of Ral GTPases regulating α-granule secretion, with RalA only playing a minor role. Further investigation into RalAB DKO α-granule secretion showed that this defect in secretion was not specific to GPVI agonists, with platelet stimulation by the PAR4-AP revealing a ~60 % reduction in P-selectin externalization – suggesting RalAB DKO platelets can sustain a moderate level of P-selectin surface expression when stimulated with high levels of a potent platelet agonist. As defects in δ-granule secretion are known to contribute to α-granule secretory defects[33], the P2Y12 blocker ARC was used to block any platelet activation by ADP released from δ-granules. Again, the defect observed without ARC was preserved, with a major reduction observed in the RalAB DKO mouse line. Integrin $\alpha_{IIb}\beta_3$ activation was not altered in any of these assays, implying that the P-selectin surface expression defect cannot be attributed to a defect in platelet activation or integrin signalling. Taken together with previous studies[19,44] the

data indicate that the α-granule secretory defects observed are likely to be due to diminished Ral-exocyst interaction.

While P-selectin surface expression was reduced, it was important to assess the release of non-membrane bound, soluble α-granule cargoes to gain a full understanding of the secretory defect. Interestingly, quantification of TGF-β and PF4 secretion from DKO platelets was largely unchanged from WT, with only TGF-β release in response to 125 μM PAR4-AP being significantly reduced by ~20 %, suggesting broadly normal cargo release (Figure 3A, B). Antibody microarray analysis of releasates isolated from stimulated WT and DKO platelets supported this, showing no alteration in the release of other known α-granule cargoes such as angiopoietin-1, endostatin, platelet derived growth factor, stromal cell-derived factor 1, thrombospondin-2, VEGF[10,45] (Supplementary Figure I). Additionally, we investigated the localisation of P-selectin in WT and DKO platelets by immunofluorescence microscopy (Figure 3C). Acquired images show similar P-selectin patterning in both WT and DKO, with P-selectin appearing to be localised to granular compartments within the platelet. Acquired TEM images of the WT and DKO platelets revealed no alteration in morphology or granule count (Supplementary Figure IIIA, B) - implying no role for Rals in controlling platelet morphology.

It was important to rule out any roles for Rals in granule biogenesis or cargo loading. Determination of relative P-selectin levels in platelet lysates by immunoblotting showed a small increase in RalAB DKO platelets compared to WT (Figure 3D). Measurement of total PF4 content by ELISA showed no difference between WT and DKO platelets, whereas TGF-β levels were slightly elevated. The data suggest that Ral GTPases play no role in platelet granule biogenesis or cargo expression.

To further investigate the α-granule secretory events occurring in RalAB DKO platelets we monitored P-selectin surface expression, integrin $\alpha_{IIb}\beta_3$ activation, PF4 release and TGF-β release over time in response to CRP-XL stimulation (Figure 4). Results revealed a substantial reduction in P-selectin surface expression over 30 minutes in RalAB DKO platelets when compared with WT (Figure 4A, Supplementary Figure IVA). Conversely, simultaneous measurement of integrin $\alpha_{IIb}\beta_3$ activation showed no difference between mouse genotypes (Figure 4B, Supplementary Figure IVB). Examining the P-selectin data shows a small increase over time in DKO P-selectin surface expression – suggesting some antibody binding to platelet P-selectin does occur upon stimulation. It is however not possible to deduce whether this antibody binding occurs upon a transient fusion event of the α-granule, where α-granule P-selectin is briefly exposed to the external milieu or if a low level of P-selectin surface expression takes place. Additionally, we observed no early appearance or spiking of the P-selectin signal in the DKO platelets in our kinetic studies (Figure 4A, Supplementary Figure IVA), which could have otherwise suggested an increased rate of P-selectin shedding or clearance. Supporting this observation, assessment of total platelet P-selectin levels after stimulation with either CRP-XL or PAR4-AP showed no reduction in P-selectin levels in WT or DKO samples (Figure 4C). This data again suggests that Ral deletion does not increase P-selectin shedding from the surface membrane, and P-

selectin is retained within/on the platelet membrane upon stimulation in both mouse lines. Finally, both PF4 and TGF-β release over 30 mins were not significantly altered by Ral deletion. Interestingly, there seems to be a disparity in the release kinetics of these two α-granule cargoes, with PF4 release peaking at 10 minutes, earlier than TGF-β release. This could be explained by PF4 being sequestered back into the platelets at a faster rate than TGF-β, or that PF4 was broken down faster than TGF-β after release. There is also the possibility of differential α-granule secretion causing a faster release of PF4 compared to TGF-β, through release from distinct subsets of α-granules[17,46].

Taken together, the absence of Ral GTPases causes an α-granule secretory defect where soluble cargoes are released, but P-selectin is not substantially expressed on the surface membrane. We believe there are two plausible explanations for these observations; (i) Rals may regulate differential secretion of α-granules with differential P-selectin content or (ii) Rals regulate kiss-and-run exocytosis where fusion of granule with target membrane is transient. Differential α-granule secretion, as described previously[17,46], could cause the secretion of different sub-populations of α-granules lacking or possessing P-selectin on their membranes. There is already evidence to suggest that P-selectin is differentially packaged from vWf in mouse platelets, indicating the presence of distinct subpopulations of P-selectin positive and negative α-granules[47]. The deletion of Ral GTPases, which localise to secretory granules[4], could therefore result in diminished secretion of P-selectin positive α-granules, but not P-selectin negative granules containing the released peptides we detected (Figure 2, Supplementary Figure I). Alternatively, the phenomenon could reflect kiss-and-run exocytosis, where a full fusion event of the secretory granule does not occur – this has previously been shown in platelets using single-cell amperometry[48,49]. Not dissimilar to chromaffin cells[50], platelet kiss-and-run exocytosis may occur upon cell stimulation and be the favoured fusion event in the absence of Ral GTPases. In this way, transient reversible fusion of α-granules with the plasma membrane may occur, but full irreversible fusion does not. This would allow for soluble cargo to be released, but α-granule membrane incorporation into the surface membrane would not occur. In a similar vein, it also plausible that Ral GTPases play a role in the docking of α-granules, comparable to a suggested role for calpain in platelets[51].

Measurement of δ-granule secretion and aggregation showed no significant difference in single Ral knockout mouse lines (Supplementary Figure V). RalAB DKO platelets did however show a small reduction in δ-granule secretion in response to sub-maximal concentrations of CRP-XL and PAR4-AP (Figure 5A), similar to the observed defect in TGF-β secretion (Figure 3B). It should also be considered that this δ-granule secretory phenotype may alter α-granule release as previously shown[33], which could explain the observed reduction in TGF-β release. Overall, our findings suggest Ral GTPases play a limited role in the regulation of δ-granule secretion, contrary to a previous study which showed that interruption of Ral-exocyst interactions in permeabilised human platelets reduced δ-granule secretion by ~70 %[19]. The difference with our study may result from the very different technical approaches used. It is also possible however that there are species differences between human and mouse platelets. The previous study does however indicate that Ral GTPases increase the sensitivity of δ-granule secretion in

response to low level platelet stimuli, which is consistent with our data, and may be mediated by a calcium-sensing role for Ral GTPases.

While the observed P-selectin and δ-granule secretory defects did not translate into reduced aggregation or thrombus formation responses (Figure 5), it is interesting to note that previous studies have implied a role for P-selectin in thrombus formation[52-54]. This may be due to a difference in models used in previous studies, where P-selectin$^{-/-}$ mice or P-selectin blocking antibodies have been used to halt P-selectin function. As the RalAB DKO mice here are generated as platelet-specific using a floxed conditional allele, endothelial cell function and endothelial P-selectin expression[55] are not disrupted – in contrast to P-selectin$^{-/-}$ mice or when using blocking antibodies. We show RalAB DKO platelets also express small amounts of surface P-selectin when stimulated with high concentrations of potent agonist (Figure 2G), suggesting P-selectin function is not completely ablated in our mice. In addition, since the major drivers of platelet aggregation and thrombus formation (integrin $\alpha_{IIb}\beta_3$ activation and δ-granule secretion[56,57]) are largely unaltered in the RalAB DKO mice, this may also help explain why arterial thrombus formation is normal in these mice.

It was important to explore the effect of reduced surface P-selectin expression on platelet-leukocyte binding (Figure 6). RalAB DKO samples showed a ~70 % reduction in the platelet-leukocyte interactions, as a result of reduced P-selectin exposure[58,59]. These results strongly indicate roles for platelet Ral GTPases in inflammatory responses, so we chose to investigate platelet Ral deletion in vivo using a DSS-induced ulcerative colitis model, due to evidence directly linking platelet α-granule secretion to IBD and Crohn's disease[60-62]. Clinical observations associated with symptoms of DSS-induced ulcerative colitis including weight loss, stool consistency/diarrhoea and presence of blood in stools were significantly reduced in RalAB DKO mice in early stages of the study (Supplementary Figure VII). This is likely to be due to reduced platelet-leukocyte interactions in the RalAB DKO mice and a subsequently slowed rate of leukocyte extravasation. Although by day 6 of the study there was no significant difference in clinical scores between RalAB WT and DKO, results from days 2 and 4 point to a role for platelet Rals in the early stages of the inflammatory process in this model. While there is evidence to suggest that the PF4 promoter model used in this study could lead to Cre expression in cells in the distal colon[63], the proportion of cells expressing Cre is not determined. With this in mind we performed an additional control experiment comparing platelet-leukocyte interactions in Cre expressing and non-expressing mice, with results showing that the presence of the Cre-PF4 promoter does not alter platelet-leukocyte interactions (Supplementary Figure VIII). It would however be ideal to include in this study mice in which Cre was selectively expressed in colon epithelial cells, but in the absence of a clean promoter system for such a study, we cannot convincingly assign phenotype solely to platelet-specific deletion of Rals. The results do however highlight the possibility that platelet-expressed Ral GTPases could be targets for the treatment of disorders associated with platelet-leukocyte interaction. Finally, these results also raise questions regarding the use of Ral inhibitors in the treatment of cancer[2], and would need further investigation if the use of these drugs significantly altered platelet or leukocyte function.

In conclusion, we have identified that platelet Ral GTPases are key regulators of P-selectin surface expression, playing only a minor role in regulating the release of soluble platelet cargoes. We propose two potential mechanisms: differential secretion of P-selectin positive α-granule subsets or kiss-and-run exocytosis. The resultant major defect in platelet P-selectin expression in the absence of RalAB induces a marked defect in platelet-leukocyte interaction. Pf4-Cre^{+} RalA/B^{flox} mice showed reduced symptoms in early stages of inflammatory bowel disease, in a mouse model system. Platelet Ral GTPases could therefore form a novel target for modulating inflammatory disease in conditions where platelet P-selectin surface expression plays an important role.

Acknowledgments

We acknowledge the MRC and the Wolfson Foundation for funding the University of Bristol's Bioimaging Facility. We are grateful to Professor Chris Marshall for his donation of $RalA^{flox/flox}$ and $RalB^{flox/flox}$ mice and for supplying the RalBP-1 GST construct. We thank Elizabeth Aitken for expert technical assistance.

Sources of funding

This work was supported by the British Heart Foundation (RG/15/16/31758, PG/14/3/30565, PG/13/11/30016, FS/14/23/30756).

Disclosures

The authors declare that no conflicts of interest exist**.**

References

1. Lim KH, O'Hayer K, Adam SJ, et al. Divergent roles for RalA and RalB in malignant growth of human pancreatic carcinoma cells. *Current biology : CB.* 2006;16(24):2385-2394.
2. Yan C, Liu D, Li L, et al. Discovery and characterization of small molecules that target the GTPase Ral. *Nature.* 2014;515(7527):443-447.
3. Thoma C. Therapy: GTPase Ral-a new tumour target. *Nat Rev Urol.* 2014;11(12):658.
4. Shirakawa R, Horiuchi H. Ral GTPases: crucial mediators of exocytosis and tumourigenesis. *J Biochem.* 2015;157(5):285-299.
5. Heider MR, Munson M. Exorcising the exocyst complex. *Traffic.* 2012;13(7):898-907.
6. Sollner T, Whiteheart SW, Brunner M, et al. SNAP receptors implicated in vesicle targeting and fusion. *Nature.* 1993;362(6418):318-324.
7. Golebiewska EM, Poole AW. Secrets of platelet exocytosis - what do we really know about platelet secretion mechanisms? *British journal of haematology.* 2013.
8. Aslan JE, McCarty OJ. Rho GTPases in platelet function. *Journal of thrombosis and haemostasis : JTH.* 2013;11(1):35-46.
9. Goggs R, Williams CM, Mellor H, Poole AW. Platelet Rho GTPases-a focus on novel players, roles and relationships. *The Biochemical journal.* 2015;466(3):431-442.
10. Maynard DM, Heijnen HF, Horne MK, White JG, Gahl WA. Proteomic analysis of platelet alpha-granules using mass spectrometry. *Journal of thrombosis and haemostasis : JTH.* 2007;5(9):1945-1955.
11. Zufferey A, Schvartz D, Nolli S, Reny JL, Sanchez JC, Fontana P. Characterization of the platelet granule proteome: evidence of the presence of MHC1 in alpha-granules. *J Proteomics.* 2014;101:130-140.
12. Meyers KM, Holmsen H, Seachord CL. Comparative study of platelet dense granule constituents. *Am J Physiol.* 1982;243(3):R454-461.
13. Golebiewska EM, Poole AW. Platelet secretion: From haemostasis to wound healing and beyond. *Blood reviews.* 2015;29(3):153-162.
14. Stenberg PE, McEver RP, Shuman MA, Jacques YV, Bainton DF. A platelet alpha-granule membrane protein (GMP-140) is expressed on the plasma membrane after activation. *The Journal of cell biology.* 1985;101(3):880-886.
15. Berman CL, Yeo EL, Wencel-Drake JD, Furie BC, Ginsberg MH, Furie B. A platelet alpha granule membrane protein that is associated with the plasma membrane after activation. Characterization and subcellular localization of platelet activation-dependent granule-external membrane protein. *The Journal of clinical investigation.* 1986;78(1):130-137.
16. White GC, 2nd, Rompietti R. Platelet secretion: indiscriminately spewed forth or highly orchestrated? *Journal of thrombosis and haemostasis : JTH.* 2007;5(10):2006-2008.
17. Sehgal S, Storrie B. Evidence that differential packaging of the major platelet granule proteins von Willebrand factor and fibrinogen can support their differential release. *Journal of thrombosis and haemostasis : JTH.* 2007;5(10):2009-2016.
18. Wolthuis RM, Franke B, van Triest M, et al. Activation of the small GTPase Ral in platelets. *Molecular and cellular biology.* 1998;18(5):2486-2491.
19. Kawato M, Shirakawa R, Kondo H, et al. Regulation of platelet dense granule secretion by the Ral GTPase-exocyst pathway. *The Journal of biological chemistry.* 2008;283(1):166-174.
20. Peschard P, McCarthy A, Leblanc-Dominguez V, et al. Genetic deletion of RALA and RALB small GTPases reveals redundant functions in development and tumorigenesis. *Current biology : CB.* 2012;22(21):2063-2068.
21. Adeghe AJ, Cohen J. A better method for terminal bleeding of mice. *Lab Anim.* 1986;20(1):70-72.
22. Goggs R, Savage JS, Mellor H, Poole AW. The small GTPase Rif is dispensable for platelet filopodia generation in mice. *PloS one.* 2013;8(1):e54663.
23. Moore SF, Williams CM, Brown E, et al. Loss of the insulin receptor in murine megakaryocytes/platelets causes thrombocytosis and alterations in IGF signalling. *Cardiovascular research.* 2015;107(1):9-19.
24. Kahr WH, Lo RW, Li L, et al. Abnormal megakaryocyte development and platelet function in Nbeal2(-/-) mice. *Blood.* 2013;122(19):3349-3358.

25. Blair TA, Moore SF, Williams CM, Poole AW, Vanhaesebroeck B, Hers I. Phosphoinositide 3-kinases p110alpha and p110beta have differential roles in insulin-like growth factor-1-mediated Akt phosphorylation and platelet priming. *Arterioscler Thromb Vasc Biol.* 2014;34(8):1681-1688.
26. Savage JS, Williams CM, Konopatskaya O, Hers I, Harper MT, Poole AW. Munc13-4 is critical for thrombosis through regulating release of ADP from platelets. *Journal of thrombosis and haemostasis : JTH.* 2013;11(4):771-775.
27. Konopatskaya O, Gilio K, Harper MT, et al. PKCalpha regulates platelet granule secretion and thrombus formation in mice. *The Journal of clinical investigation.* 2009;119(2):399-407.
28. Polakis PG, Weber RF, Nevins B, Didsbury JR, Evans T, Snyderman R. Identification of the ral and rac1 gene products, low molecular mass GTP-binding proteins from human platelets. *The Journal of biological chemistry.* 1989;264(28):16383-16389.
29. Vega IE, Hsu SC. The exocyst complex associates with microtubules to mediate vesicle targeting and neurite outgrowth. *The Journal of neuroscience : the official journal of the Society for Neuroscience.* 2001;21(11):3839-3848.
30. Wang S, Liu Y, Adamson CL, Valdez G, Guo W, Hsu SC. The mammalian exocyst, a complex required for exocytosis, inhibits tubulin polymerization. *The Journal of biological chemistry.* 2004;279(34):35958-35966.
31. Gromley A, Yeaman C, Rosa J, et al. Centriolin anchoring of exocyst and SNARE complexes at the midbody is required for secretory-vesicle-mediated abscission. *Cell.* 2005;123(1):75-87.
32. Rowley JW, Oler AJ, Tolley ND, et al. Genome-wide RNA-seq analysis of human and mouse platelet transcriptomes. *Blood.* 2011;118(14):e101-111.
33. Harper MT, van den Bosch MT, Hers I, Poole AW. Platelet dense granule secretion defects may obscure alpha-granule secretion mechanisms: evidence from Munc13-4-deficient platelets. *Blood.* 2015;125(19):3034-3036.
34. Yang J, Furie BC, Furie B. The biology of P-selectin glycoprotein ligand-1: its role as a selectin counterreceptor in leukocyte-endothelial and leukocyte-platelet interaction. *Thrombosis and haemostasis.* 1999;81(1):1-7.
35. Zarbock A, Polanowska-Grabowska RK, Ley K. Platelet-neutrophil-interactions: linking hemostasis and inflammation. *Blood reviews.* 2007;21(2):99-111.
36. Lam FW, Vijayan KV, Rumbaut RE. Platelets and Their Interactions with Other Immune Cells. *Compr Physiol.* 2015;5(3):1265-1280.
37. Schmitt-Sody M, Metz P, Gottschalk O, et al. Platelet P-selectin is significantly involved in leukocyte-endothelial cell interaction in murine antigen-induced arthritis. *Platelets.* 2007;18(5):365-372.
38. Yan SL, Russell J, Granger DN. Platelet activation and platelet-leukocyte aggregation elicited in experimental colitis are mediated by interleukin-6. *Inflamm Bowel Dis.* 2014;20(2):353-362.
39. Chassaing B, Aitken JD, Malleshappa M, Vijay-Kumar M. Dextran sulfate sodium (DSS)-induced colitis in mice. *Curr Protoc Immunol.* 2014;104:Unit 15 25.
40. Vowinkel T, Anthoni C, Wood KC, et al. CD40-CD40 ligand mediates the recruitment of leukocytes and platelets in the inflamed murine colon. *Gastroenterology.* 2007;132(3):955-965.
41. Gironella M, Molla M, Salas A, et al. The role of P-selectin in experimental colitis as determined by antibody immunoblockade and genetically deficient mice. *J Leukoc Biol.* 2002;72(1):56-64.
42. Yu C, Zhang S, Wang Y, Zhang S, Luo L, Thorlacius H. Platelet-Derived CCL5 Regulates CXC Chemokine Formation and Neutrophil Recruitment in Acute Experimental Colitis. *J Cell Physiol.* 2016;231(2):370-376.
43. Wu B, Guo W. The Exocyst at a Glance. *Journal of cell science.* 2015;128(16):2957-2964.
44. Moskalenko S, Henry DO, Rosse C, Mirey G, Camonis JH, White MA. The exocyst is a Ral effector complex. *Nature cell biology.* 2002;4(1):66-72.
45. Jonnalagadda D, Izu LT, Whiteheart SW. Platelet secretion is kinetically heterogeneous in an agonist-responsive manner. *Blood.* 2012;120(26):5209-5216.
46. Italiano JE, Jr., Battinelli EM. Selective sorting of alpha-granule proteins. *Journal of thrombosis and haemostasis : JTH.* 2009;7 Suppl 1:173-176.
47. Zingariello M, Fabucci ME, Bosco D, et al. Differential localization of P-selectin and von Willebrand factor during megakaryocyte maturation. *Biotech Histochem.* 2010;85(3):157-170.
48. Fitch-Tewfik JL, Flaumenhaft R. Platelet granule exocytosis: a comparison with chromaffin cells. *Front Endocrinol (Lausanne).* 2013;4:77.

49. Ge S, Woo E, Haynes CL. Quantal regulation and exocytosis of platelet dense-body granules. *Biophysical journal.* 2011;101(10):2351-2359.
50. Elhamdani A, Azizi F, Artalejo CR. Double patch clamp reveals that transient fusion (kiss-and-run) is a major mechanism of secretion in calf adrenal chromaffin cells: high calcium shifts the mechanism from kiss-and-run to complete fusion. *The Journal of neuroscience : the official journal of the Society for Neuroscience.* 2006;26(11):3030-3036.
51. Croce K, Flaumenhaft R, Rivers M, et al. Inhibition of calpain blocks platelet secretion, aggregation, and spreading. *The Journal of biological chemistry.* 1999;274(51):36321-36327.
52. Subramaniam M, Frenette PS, Saffaripour S, Johnson RC, Hynes RO, Wagner DD. Defects in hemostasis in P-selectin-deficient mice. *Blood.* 1996;87(4):1238-1242.
53. Downing LJ, Wakefield TW, Strieter RM, et al. Anti-P-selectin antibody decreases inflammation and thrombus formation in venous thrombosis. *J Vasc Surg.* 1997;25(5):816-827; discussion 828.
54. Prakash P, Nayak MK, Chauhan AK. P-selectin can promote thrombus propagation independently of both von Willebrand factor and thrombospondin-1 in mice. *Journal of thrombosis and haemostasis : JTH.* 2017;15(2):388-394.
55. Yau JW, Teoh H, Verma S. Endothelial cell control of thrombosis. *BMC cardiovascular disorders.* 2015;15:130.
56. Jackson SP, Nesbitt WS, Westein E. Dynamics of platelet thrombus formation. *Journal of thrombosis and haemostasis : JTH.* 2009;7 Suppl 1:17-20.
57. Stoll G, Kleinschnitz C, Nieswandt B. Molecular mechanisms of thrombus formation in ischemic stroke: novel insights and targets for treatment. *Blood.* 2008;112(9):3555-3562.
58. McEver RP. Adhesive interactions of leukocytes, platelets, and the vessel wall during hemostasis and inflammation. *Thrombosis and haemostasis.* 2001;86(3):746-756.
59. Kling D, Stucki C, Kronenberg S, et al. Pharmacological control of platelet-leukocyte interactions by the human anti-P-selectin antibody inclacumab--preclinical and clinical studies. *Thrombosis research.* 2013;131(5):401-410.
60. Danese S, Katz JA, Saibeni S, et al. Activated platelets are the source of elevated levels of soluble CD40 ligand in the circulation of inflammatory bowel disease patients. *Gut.* 2003;52(10):1435-1441.
61. Danese S, Motte Cd Cde L, Fiocchi C. Platelets in inflammatory bowel disease: clinical, pathogenic, and therapeutic implications. *Am J Gastroenterol.* 2004;99(5):938-945.
62. Aukrust P, Damas JK, Solum NO. Soluble CD40 ligand and platelets: self-perpetuating pathogenic loop in thrombosis and inflammation? *Journal of the American College of Cardiology.* 2004;43(12):2326-2328.
63. Pertuy F, Aguilar A, Strassel C, et al. Broader expression of the mouse platelet factor 4-cre transgene beyond the megakaryocyte lineage. *Journal of thrombosis and haemostasis : JTH.* 2015;13(1):115-125.

Highlights:

- Genetic deletion of RalA and RalB GTPases in mouse platelets highlights a major role for Rals in regulating the surface expression of α-granule P-selectin, but not in the release of soluble α-granule cargo.
- Diminished P-selectin surface expression leads to a reduction in the formation of platelet-leukocyte interactions *in vitro*. In an *in vivo* mouse model of inflammatory bowel disease (DSS-induced ulcerative colitis) onset of the pathology is delayed in Pf4-Cre^{+} RalA/B^{flox} mice.
- Ral GTPases could be important novel targets for the selective control of platelet-mediated immune cell recruitment and inflammatory disease.

Figures

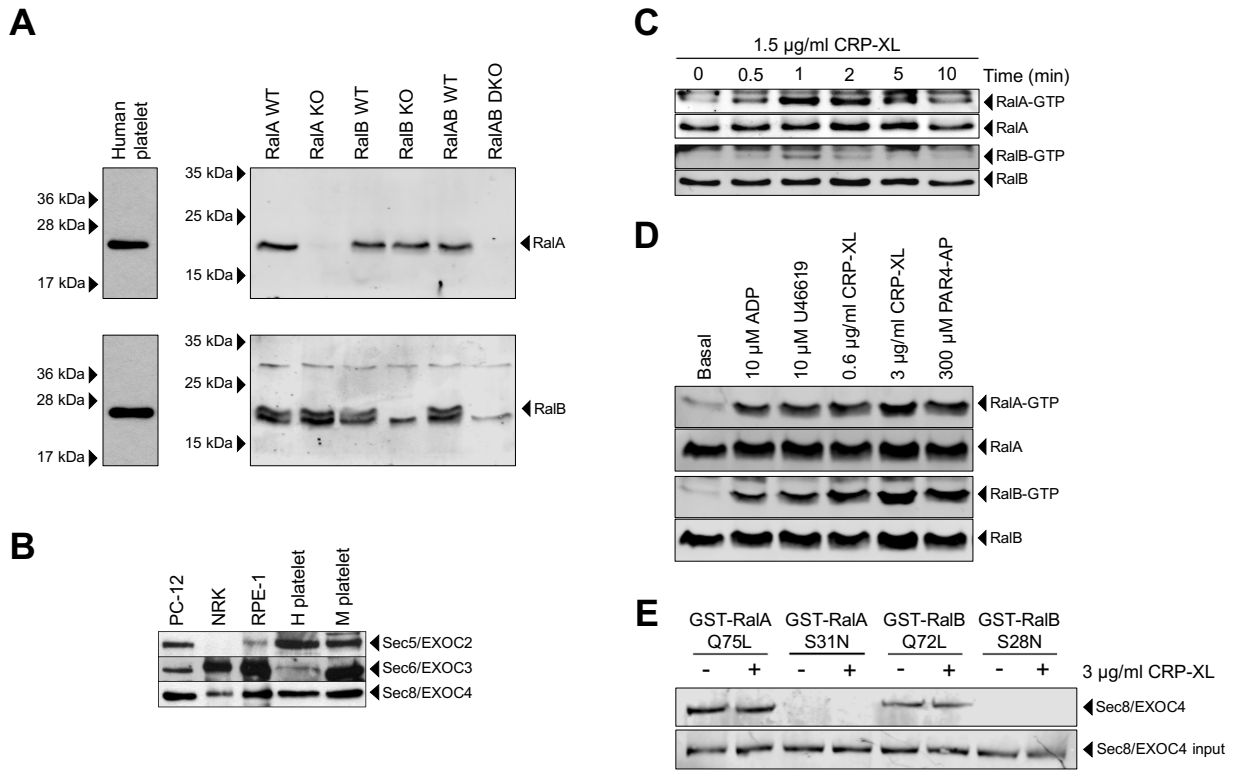

Figure 1. Ral GTPases and the exocyst complex in platelets. (A) Platelet lysates (4 x 10^8 platelets/mL) from human and mouse (wild type (WT) or genetically modified as indicated) were probed for the presence of RalA and RalB GTPases. (B) Control cell lysates from PC-12, NRK and RPE-1 (2.5 mg/ml) were probed for exocyst components Sec5, Sec6 and Sec8 alongside human and murine platelet lysates (4 x 10^8 platelets/mL). (C) Human platelets were isolated and stimulated with 1.5 µg/mL CRP-XL for the times indicated. RalBP1-GST bead pull-downs, to recover active (GTP-bound) Rals, were blotted for RalA (RalA-GTP row) or RalB (RalB-GTP row). Input lysates were blotted for RalA and RalB, as loading controls, as shown. (D) Human platelets were isolated and stimulated for 1 min with agonists indicated, lysed and incubated with RalBP1-GST beads to precipitate active Rals. Pull-downs were blotted for RalA (RalA-GTP row) or RalB (RalB-GTP row). Input lysates were blotted for RalA and RalB, as loading controls, as shown. (E) Human platelets were isolated and stimulated with 3 µg/mL CRP-XL for 1 minute prior to lysis and incubation with constitutively active (Q75L, Q72L) or inactive (S31N, S28N) mutant forms of RalA/B-GST beads. Proteins were eluted and probed for the exocyst component Sec8. Data shown are representative of 3 independent experiments.

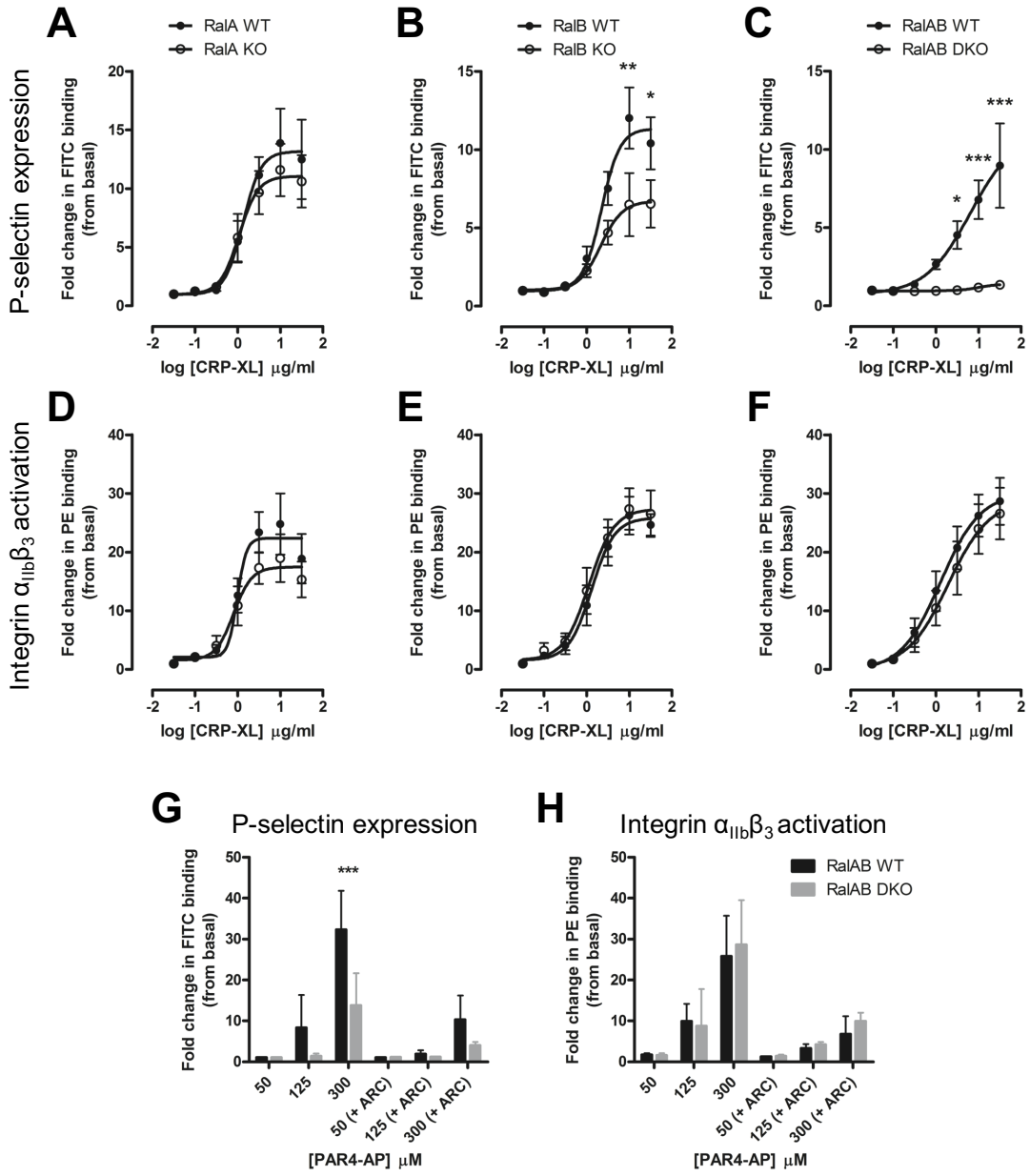

Figure 2. Ral GTPases regulate P-selectin expression on the surface membrane. Flow cytometry was used to determine P-selectin expression on the surface membrane (A-C, G) and integrin $\alpha_{IIb}\beta_3$ activation (D-F, H) in RalA WT/KO (A, D), RalB WT/KO (B, E) and RalAB WT/DKO (C, F, G, H). Mouse platelets (5 x 10^7 platelets/mL) were incubated with PE-conjugated anti-integrin $\alpha_{IIb}\beta_3$ and FITC-conjugated anti-CD62P/P-selectin antibodies before stimulation with indicated concentrations of CRP-XL (A-F) and PAR4-AP. For some experiments, shown in G & H, platelets were pretreated with 10 μM ARC for 10 min. Data for A-F are mean values ± SEM (n=7) and G, H are mean values ± SEM (n=4). Statistical analysis was performed by 2-way ANOVA with Bonferroni's post-hoc test (*** = $p < 0.001$, ** = $p < 0.01$, * = $p < 0.05$).

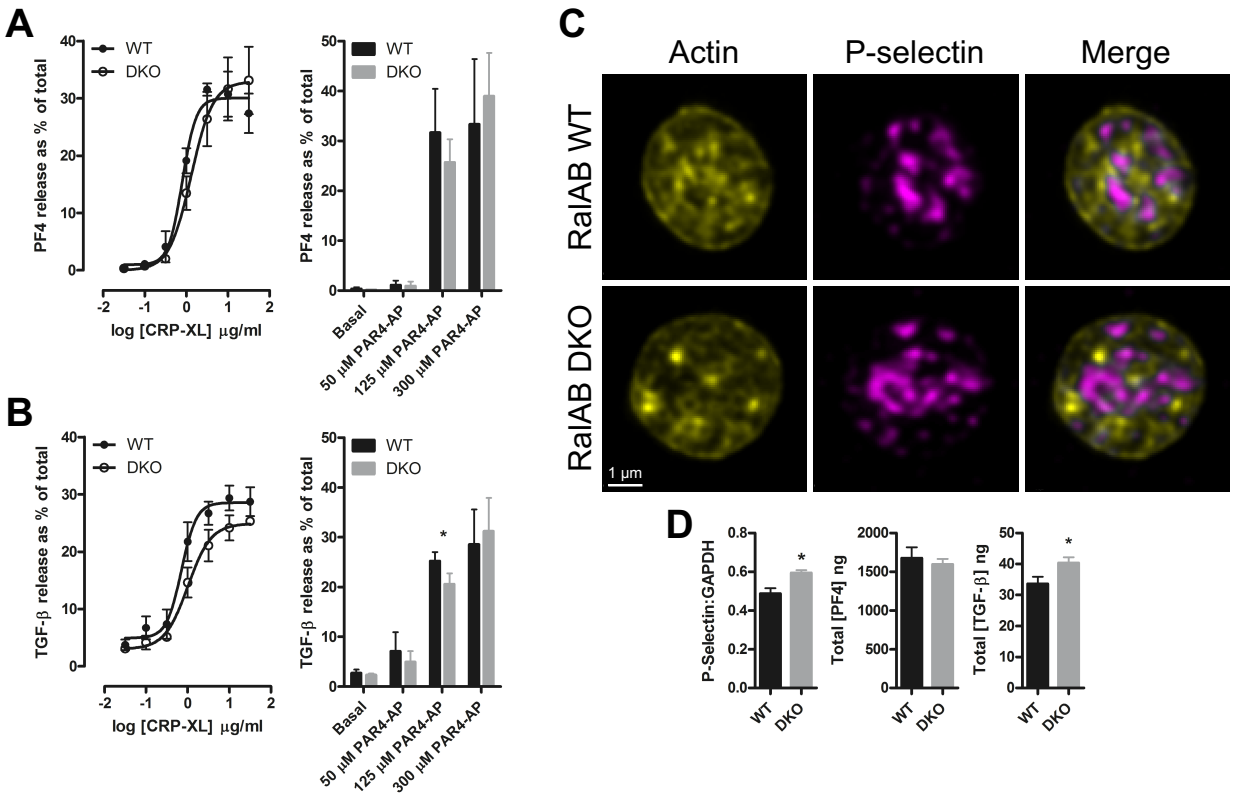

Figure 3. Ral deletion marginally alters α-granule cargo levels and release. Secretion of PF4 (A) and TGF-β (B) from CRP-XL and PAR4-AP-stimulated RalAB WT and DKO platelets (2 x 10^8 platelets/mL) was determined by ELISA and are displayed as a percentage release of total platelet content. Platelets were stimulated with indicated concentrations of agonist before releasates were isolated by centrifugation of samples at 650 *g* for 1 min. Data shown are mean ± SEM (n=5), statistical analysis – 2-way ANOVA with Bonferroni's post-hoc test (* = p <0.05). (C) Platelets were isolated from RalAB WT and DKO mice and fixed before spotting on coverslips and permeabilisation with 0.2 % Triton-X. Samples were immunostained with ActinGreen (yellow) and goat anti-mouse P-selectin and anti-goat Alexafluor 642 (magenta). Samples were visualised by confocal microscopy, with multiple z-stacks shown in extended focus. Images are representative of 3 separate experiments (n=3). Scale bar is equal to 1 µm. (D) Total P-selectin content relative to GAPDH in platelet lysates was determined by western blotting and densitometry. Total TGF-β and PF4 content was determined by ELISA. Bars represent mean ± SEM (n=3-5). Statistical analysis was performed by unpaired t-test (* = p < 0.05).

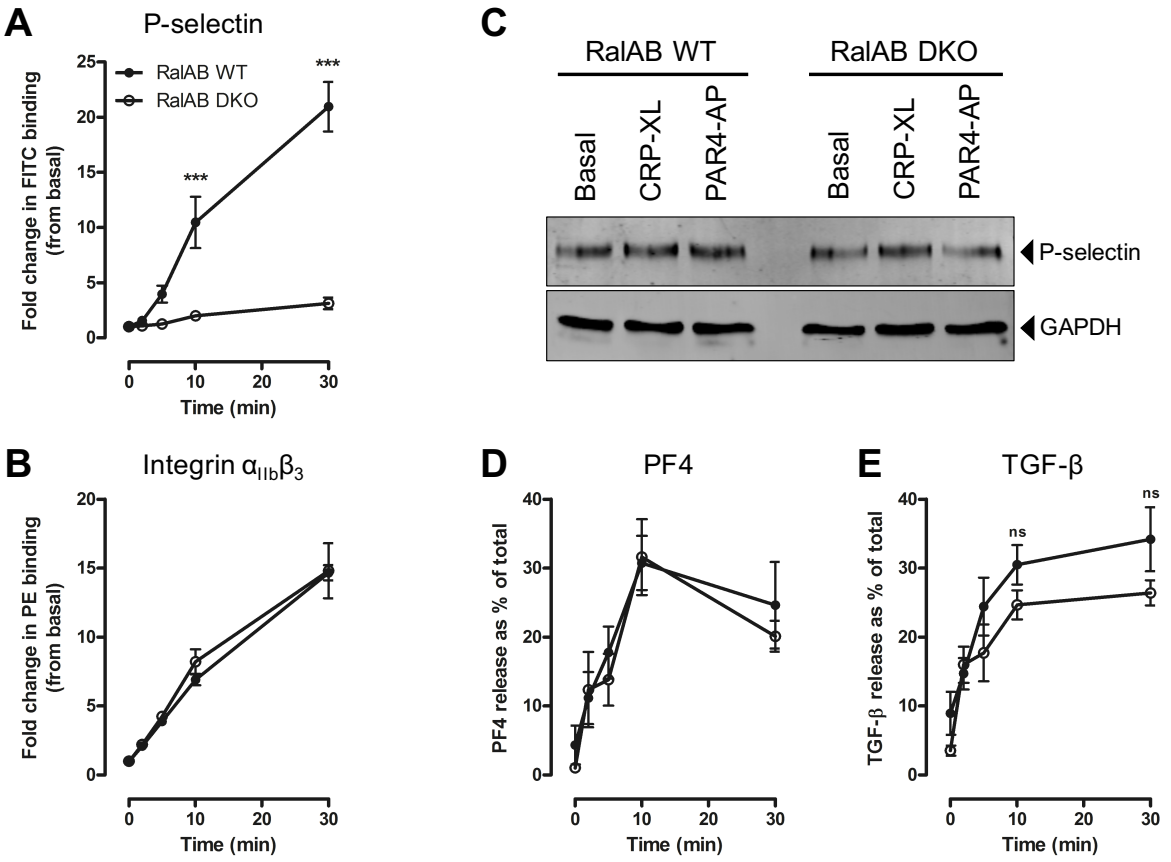

Figure 4. Investigating the kinetics of α-granule secretion in RalAB WT and DKO platelets. Flow cytometry was used to determine P-selectin expression on the surface membrane (A) and integrin $\alpha_{IIb}\beta_3$ activation (B) in RalAB WT/DKO platelets over a 30 minutes period. Mouse platelets (5 x 10^7 platelets/ml) were incubated with PE-conjugated anti-integrin $\alpha_{IIb}\beta_3$ and FITC-conjugated anti-CD62P/P-selectin antibodies before stimulation with 3 µg/ml CRP-XL. Sample were then fixed with an equal volume of 2 % PFA after 0, 2, 5, 10 and 30 minutesof stimulation. (C) Platelet P-selectin levels after stimulation were determined by western blotting. Platelets (4 x 10^8 platelets/ml) from RalAB WT and DKO mice were stimulated with 3 µg/ml CRP-XL or 125 µM PAR4-AP for 10 minutes before isolation by centrifugation. Supernatant was removed before pelleted platelets were resuspended and lysed. Platelet lysates were then probed for P-selectin, with GAPDH used as a loading control. Secretion of PF4 (D) and TGF-β (E) from RalAB WT and DKO platelets (2 x 10^8 platelets/mL) over 30 minutes was determined by ELISA and are displayed as a percentage release of total platelet content. Platelets were stimulated with 3 µg/ml CRP-XL for 0, 2, 5, 10 and 30 minute before samples were centrifuged at 650 g for 1 min and releasates collected. Kinetic data (A, B, D, E) are mean ± SEM (n=5) with statistical analysis performed by 2-way ANOVA with Bonferroni's post-hoc test (*** = $p < 0.001$). Blot image (C) is representative of 3 independent experiments (n=3).

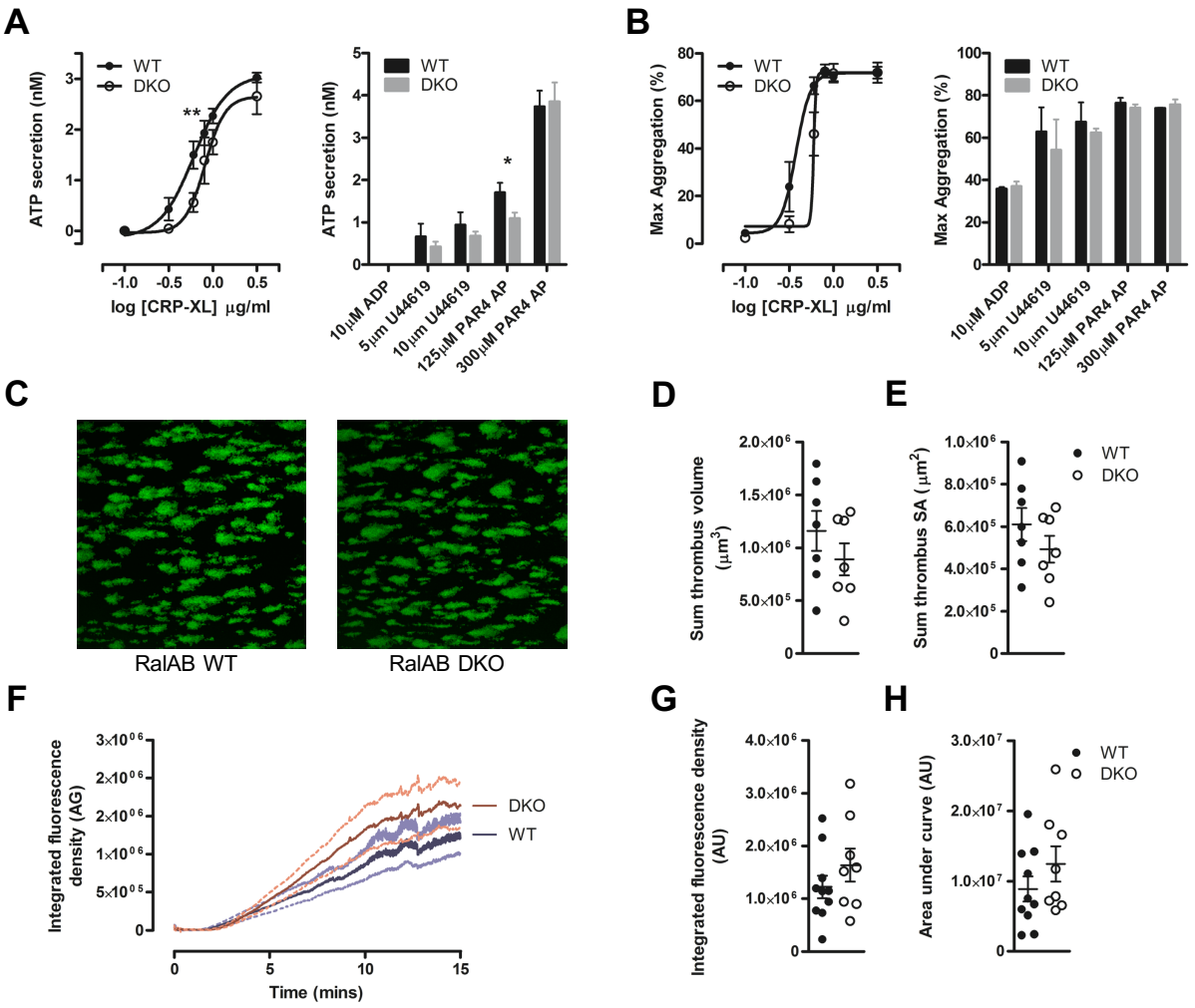

Figure 5. Deletion of Ral GTPases does not alter aggregation or thrombus formation. ATP secretion (A) and max aggregation (B) were determined simultaneously by lumi-aggregometry. Mouse platelets (2 x 10^8 platelets/mL, from either RalAB WT or DKO mice were stimulated with indicated concentrations of CRP-XL, ADP, U44619 and PAR4-AP for 5 min with constant stirring. (C) Whole blood from RalAB WT and DKO mice was incubated with 2 µM $DiOC_6$ before being flowed through a collagen-coated chamber (1000 s^{-1} for 2 min). Adherent platelets were fixed and representative images shown. Quantification of total thrombus volume (µm^3) (D) and surface area covered (µm^2) (E) is also shown. (F) A ferric chloride carotid injury model (described in Methods) was used to evaluate *in vivo* thrombus formation real-time in RalAB WT and DKO mice. Accumulation of fluorescently labelled platelets at the site of injury is shown by mean integrated fluorescence over 15 min (F), endpoint (at 15 min) integrated fluorescence (G) and area under curve (at 15 min, H). For (A, B) data are mean values ± SEM (n=4-7); statistical analysis – 2-way ANOVA with Bonferroni's post-hoc test (** = $p < 0.01$, * = $p < 0.05$). For (C-E) data are mean values ± SEM (n=7); statistical analysis – unpaired t-test. For (F-H) data are mean values ± SEM (n=9); statistical analysis – unpaired t-test. Unpaired t-tests (D, E, G, H) found no significant difference between WT and DKO.

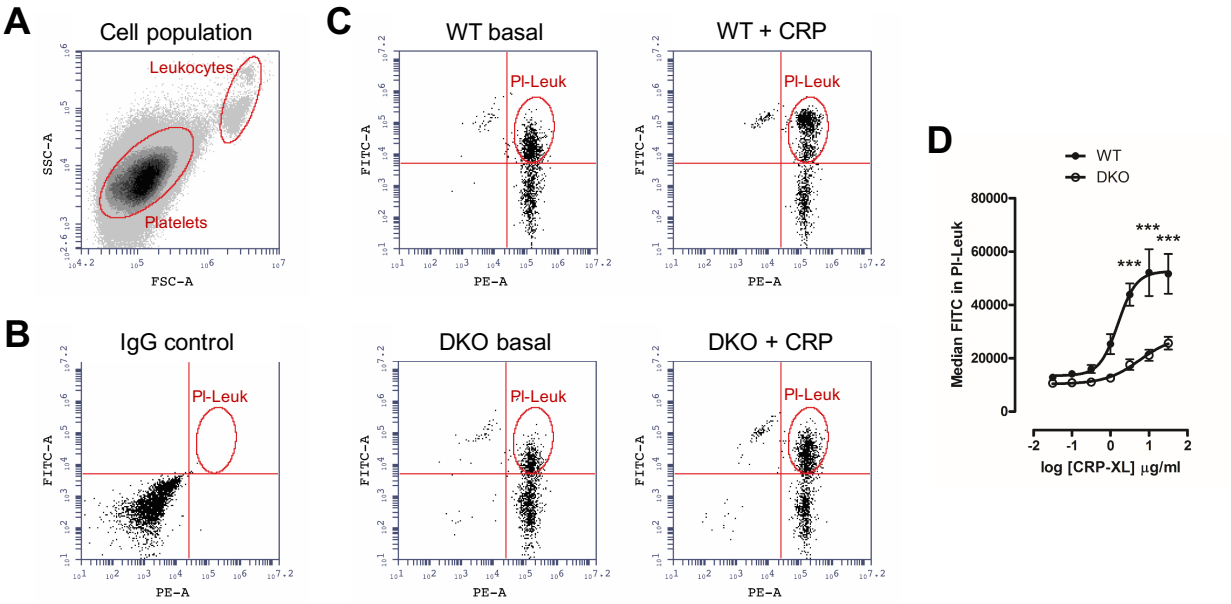

Figure 6. Platelet-leukocyte interactions are reduced in RalAB DKO mice compared with RalAB WT. Whole blood isolated from RalAB WT and DKO mice was subject to RBC lysis before stimulation with various concentrations of CRP-XL for 10 min. Samples were then stained with PE-conjugated anti-CD45 and FITC-conjugated anti-CD41. (A) Representative scatter plot showing platelet and leukocyte regions/gates post sample RBC lysis. (B) IgG antibody controls were used to generate quadrants determining specific antibody binding within the leukocytes gate. (C) FITC vs PE plots for basal and stimulated (10 µg/ml CRP-XL) WT/DKO samples within the leukocytes gate. Events detected within the top right quadrant signified events positive for both FITC (CD41) and PE (CD45) – indicating platelet-leukocyte (Pl-Leuk) aggregates. (D) Median FITC fluorescence within the Pl-Leuk gate. For A-C, data shown are representative of 5 independent experiments. For D, data are mean values ± SEM (n=5). Statistical analysis was performed by 2-way ANOVA with Bonferroni's post-hoc test (*** = $p <$ 0.001).

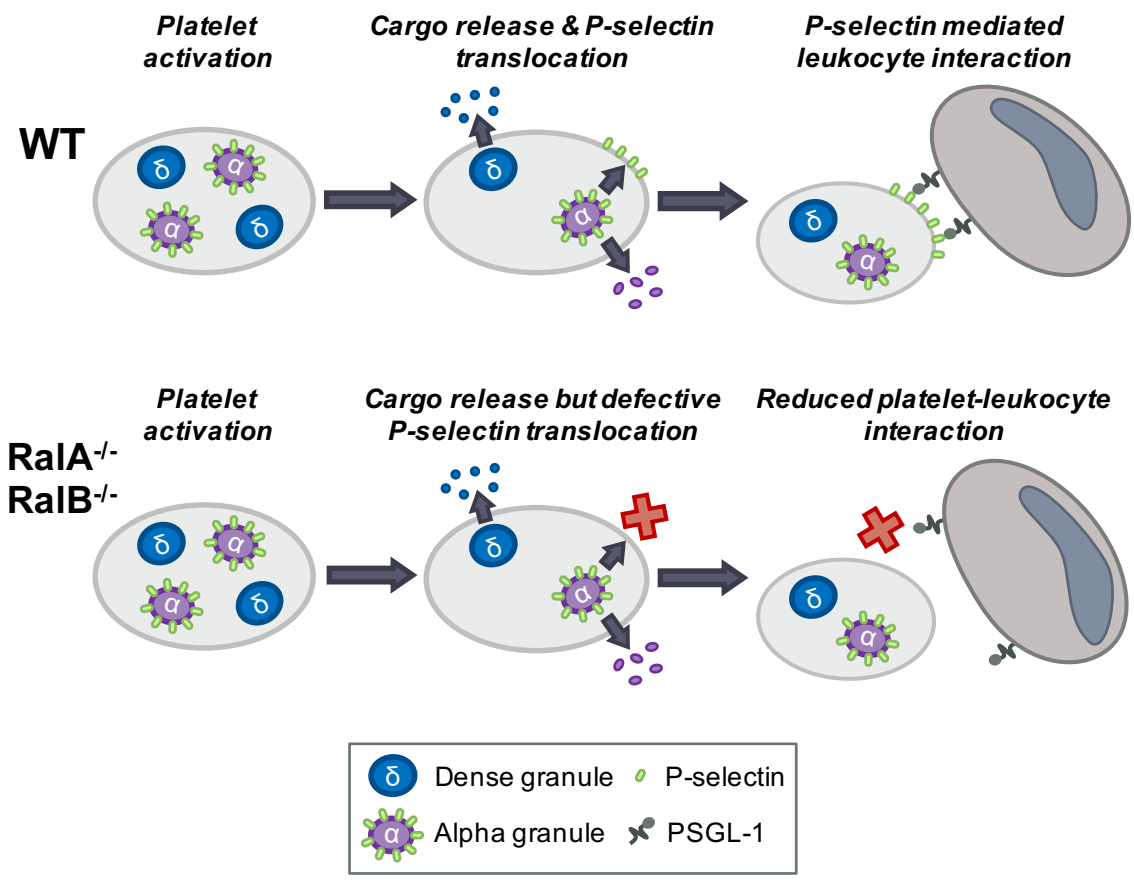
Platelet activation
Cargo release & P-selectin translocation
P-selectin mediated leukocyte interaction
WT
Platelet activation
Cargo release but defective P-selectin translocation
Reduced platelet-leukocyte interaction
RalA-/-
RalB-/-
Dense granule
P-selectin
Alpha granule
PSGL-1

Supplemental Figures

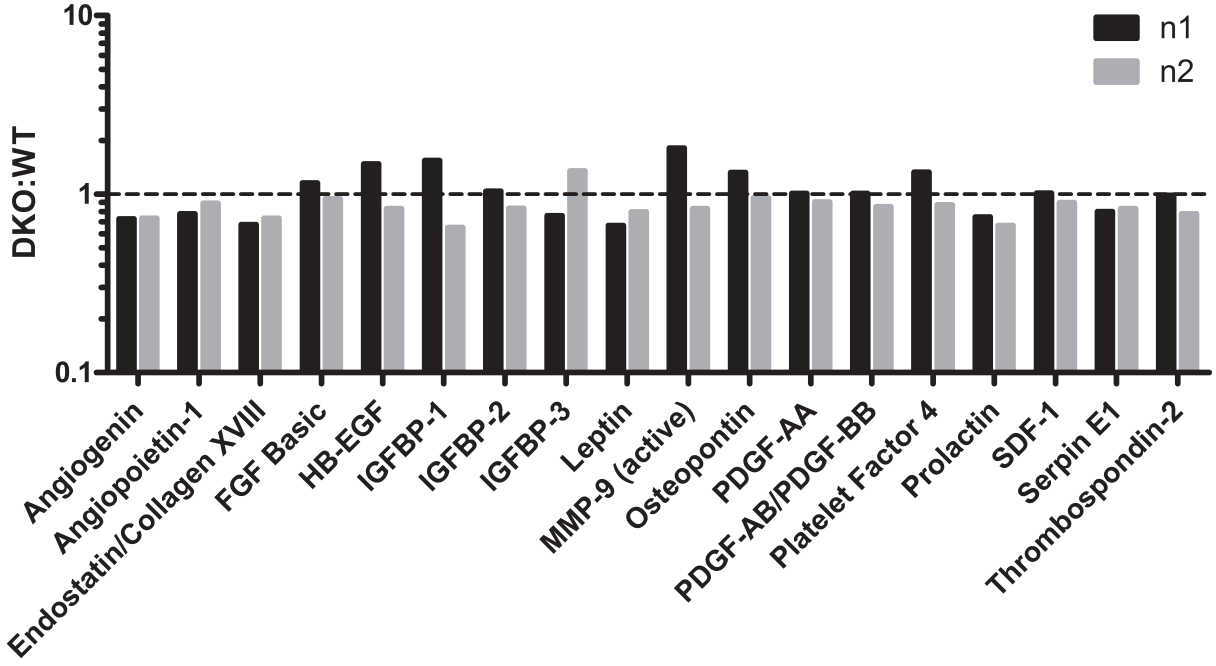

Supplementary Figure I. Ral deletion does not alter α-granule content release. Releasates from RalAB WT and DKO platelets stimulated with CRP-XL (3 μg/mL) were probed for angiogenesis-related proteins by antibody microarray. Bars represent relative protein abundance as a DKO:WT ratio; data are means from two separate pairs of mice (n=2).

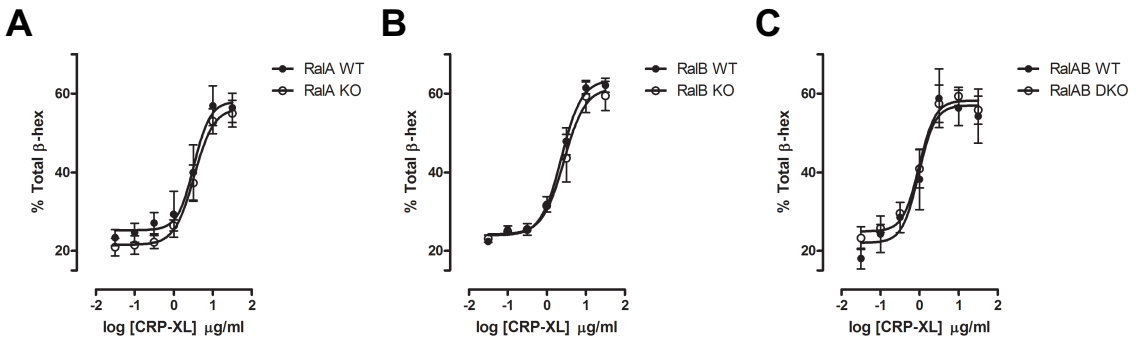

Supplementary Figure II. Ral deletion does not alter lysosomal secretion. RalA WT/KO (A), RalB WT/KO (B) and RalAB WT/DKO (C) platelets (2 x 10^8 platelets/ml) were stimulated with indicated concentrations of CRP-XL for 10 min before collection of releasates by centrifugation. Releasates were probed for β-hexosaminidase by incubation with P-NAG for 2 hours before quenching of the reaction with NaOH. Concentration of β-hexosaminidase was determined by colorimetric readout, with a lysed platelet control used as a total control. Data shown are mean ± SEM (n=3), statistical analysis was performed by 2-way ANOVA with Bonerroni's post-hoc test, with no difference found between mouse lines.

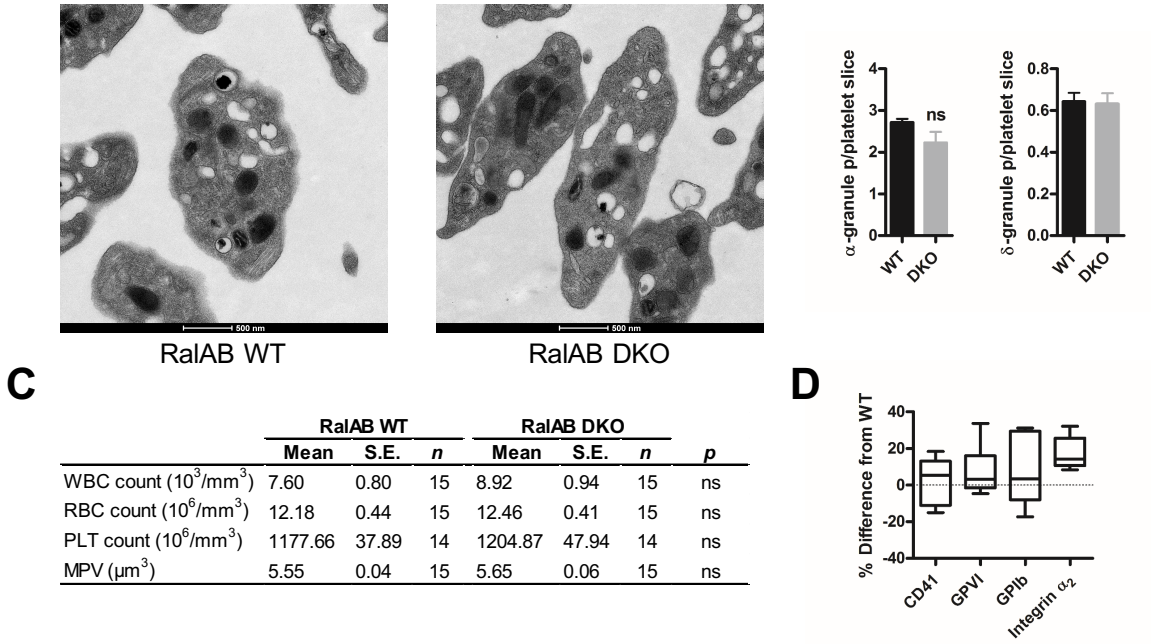

	RalAB WT			RalAB DKO			
	Mean	**S.E.**	***n***	**Mean**	**S.E.**	***n***	***p***
WBC count (10^3/mm^3)	7.60	0.80	15	8.92	0.94	15	ns
RBC count (10^6/mm^3)	12.18	0.44	15	12.46	0.41	15	ns
PLT count (10^6/mm^3)	1177.66	37.89	14	1204.87	47.94	14	ns
MPV (μm^3)	5.55	0.04	15	5.65	0.06	15	ns

Supplementary Figure III. Deletion of platelet Ral GTPases does not alter platelet count, receptor expression or morphology. Representative TEM images of RalAB WT and DKO platelets are shown (A) and quantified in (B). Numbers of platelet α- and δ-granules were evaluated from 3 pairs of mice, where granules were counted in 15 equivalent-sized fields of view. Statistical analysis by unpaired t-test showed no significant difference in granule numbers between WT and DKO. Bars represent mean values ± SEM (n=3). (C) Haematology values for whole blood isolated from RalAB WT and DKO mice. Data show mean, SEM, n values and statistical significance (p value) for differences between WT and DKO, for white blood cell count (WBC), red blood cell count (RBC), platelet count (PLT) and mean platelet volume (MPV) as indicated. (D) Surface expression of key platelet glycoproteins was determined by FACS on RalAB WT and DKO mouse platelets. Data are shown as % difference of DKO from WT values, with boxes representing mean values extending to 25th and 75th percentiles and whiskers representing max-min values (n=6). 2-way ANOVA with Bonferroni's post-hoc showed no difference in glycoprotein surface expression between WT and DKO.

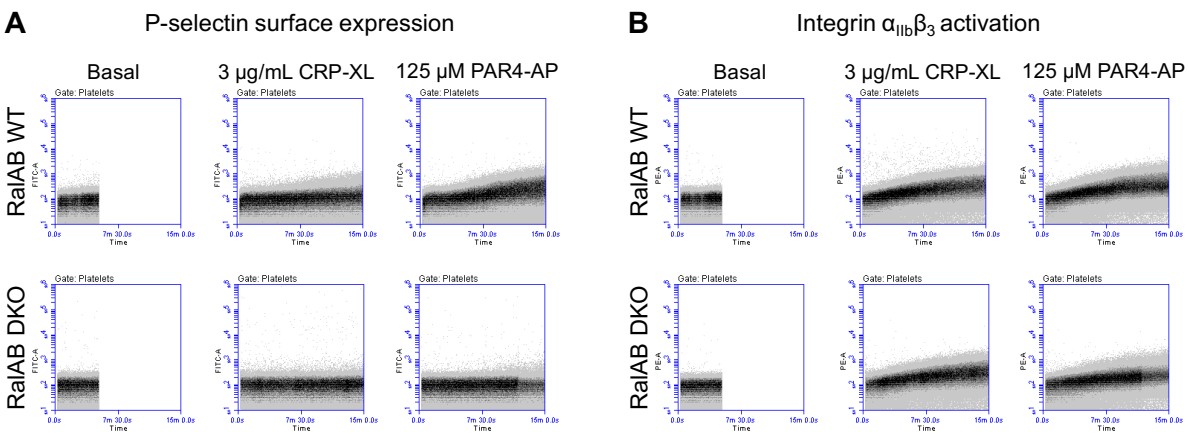

Supplementary Figure IV. Real-time determination of P-selectin surface expression and integrin $\alpha_{IIb}\beta_3$ activation in RalAB WT and DKO platelets. Flow cytometry was used to simultaneously visualise the kinetics of P-selectin expression on the surface membrane (A) and integrin $\alpha_{IIb}\beta_3$ activation (B) in RalAB WT and DKO platelets. Mouse platelets (2×10^6 platelets/ml) were incubated with FITC-conjugated anti-CD62P/P-selectin and PE-conjugated anti-integrin $\alpha_{IIb}\beta_3$ and stimulated with indicated concentrations of agonist (final sample volume 300 µl). Samples were immediately analysed by flow cytometry for 15 minutes at a flow rate of 14 µl/min. Plots are representative of 3 separate mouse pairs (n=3).

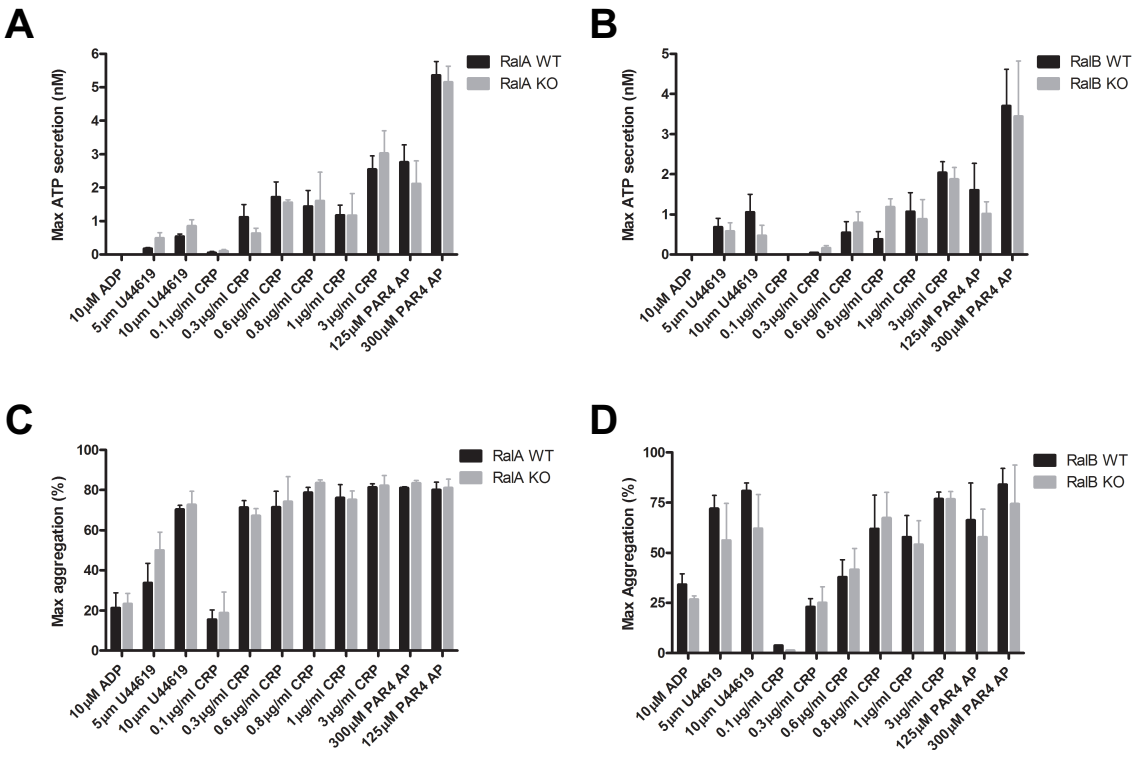

Supplementary Figure V. Individual RalA or RalB deletion does not alter δ-granule secretion or aggregation. ATP secretion and max aggregation in RalA WT/KO (A,C) and RalB WT/KO (B,D) platelets were determined simultaneously by lumi-aggregometry. Mouse platelets (2 x 10^8 platelets/mL) were stimulated with indicated concentrations of CRP-XL, ADP, U44619 and PAR4-AP for 5 min with constant stirring. Data represent mean values ± SEM (n=4-7), statistical analysis – 2-way ANOVA with Bonferroni's post-hoc test.

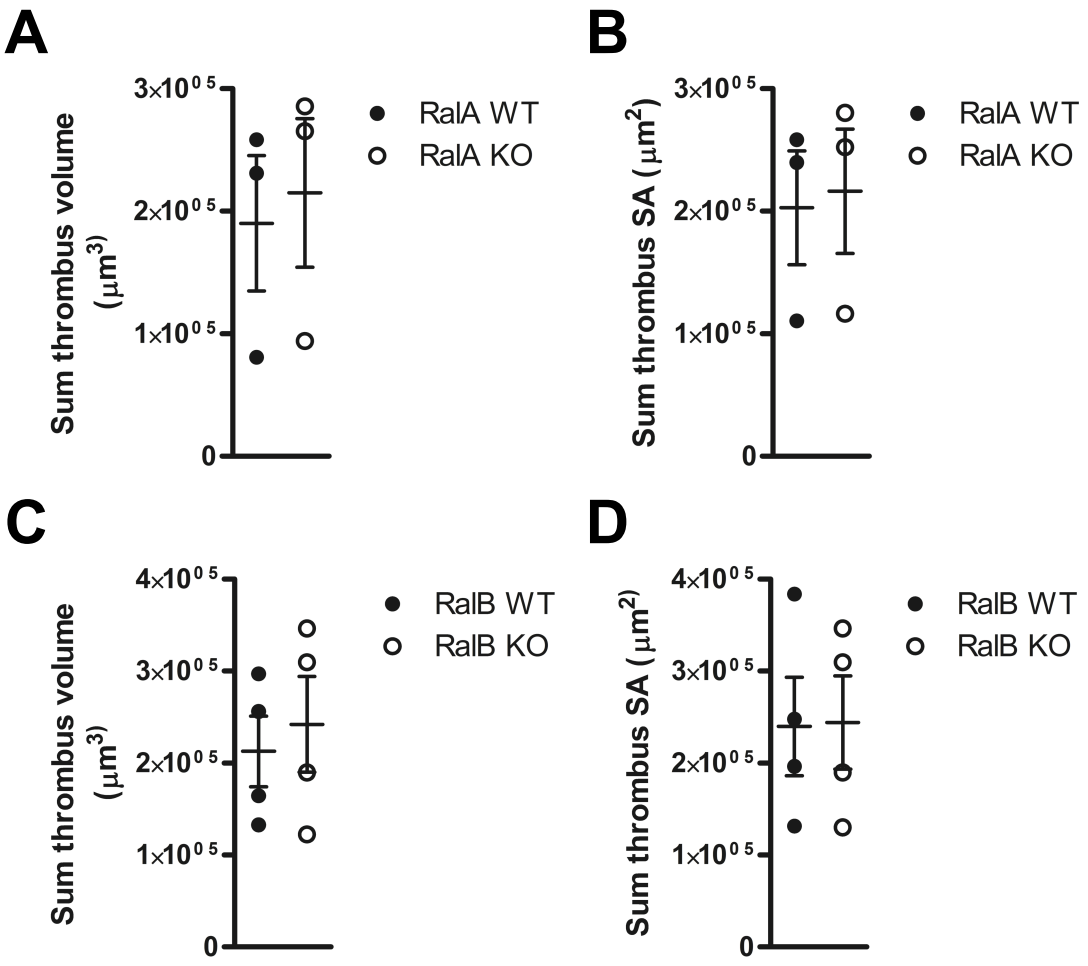

Supplementary Figure VI. Individual RalA or RalB deletion does not alter thrombus formation *in* vitro. Blood isolated from RalA WT/KO (A,B) and RalB WT/KO (C,D) mice was incubated with 2 μM $DiOC_6$ before being flowed through a collagen-coated chamber (1000 s^{-1} for 2 min). Adherent platelets were fixed and representative images shown. Quantification of total thrombus volume (μm^3) and surface area covered (μm^2) was achieved with Volocity image analysis software. Statistical analysis was performed by unpaired t-test, with no significant difference found between Ral WT and Ral KO mouse lines.

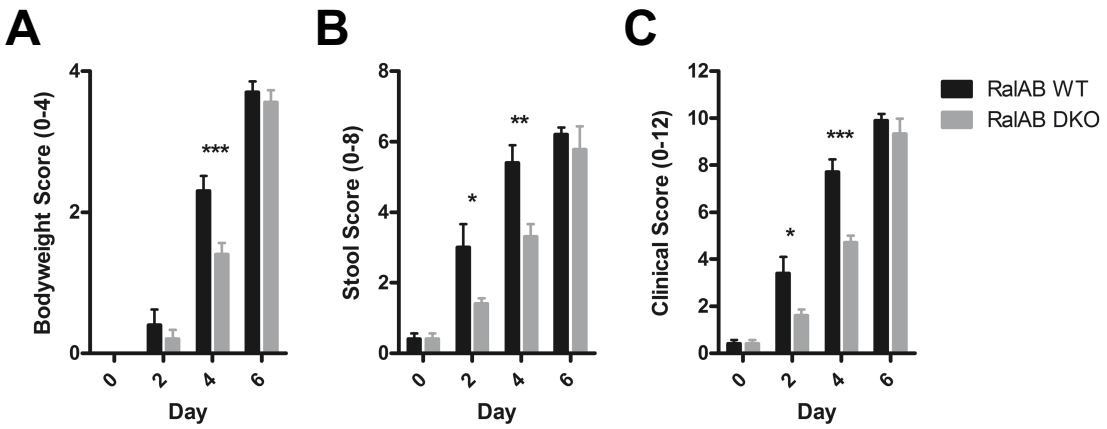

Supplementary Figure VII. Symptoms of DSS-induced ulcerative colitis are delayed in RalAB DKO mice when compared to WT. The drinking water of 10 RalAB WT and DKO age matched (8-10 week) pairs was replaced with 5 % DSS. Changes in mouse bodyweight were recorded, allowing for calculation of a bodyweight score (A) [0 % weight loss - 0, 1-5 % weight loss - 1, 5-10% - 2, 10-15 % - 3, >15 % - 4]. Stool scores (B) were generated by monitoring consistency and presence of blood in stools. Consistency of stools was ranked on a scale of 0-4, with 0 being normal and 4 being diarrhoea. Likewise, presence of blood in stools was ranked on a scale of 0-4, with 0 being no blood and 4 being gross bleeding. The sum of consistency and blood presence scores represents the overall stool score (B). The overall clinical score (C) represents the sum of both bodyweight and stool scores, used as an overall measure of the progression of the DSS-induced ulcerative colitis model. Bars represent mean values ± SEM (n=10). Statistical analysis was performed by 2-way ANOVA (*** = $p < 0.001$, ** = $p < 0.01$, * = $p < 0.05$).

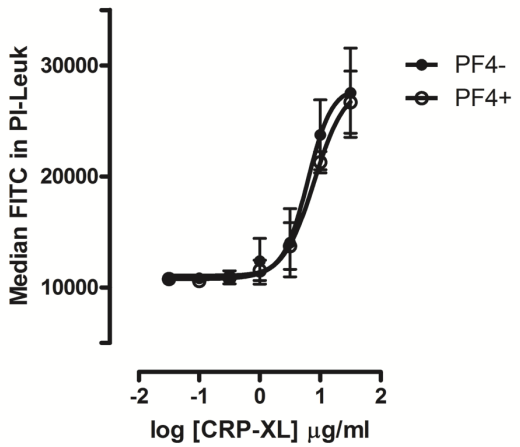

Supplementary Figure VIII. The expression of a Cre-PF4 promoter does not alter platelet-leukocyte interactions. Whole blood isolated from Cre-PF4- and Cre-PF4+ mice was subject to RBC lysis before stimulation with various concentrations of CRP-XL for 10 min. Samples were then stained with PE-conjugated anti-CD45 and FITC-conjugated anti-CD41. IgG antibody controls were used to generate quadrants determining specific antibody binding within the leukocyte population. Data are mean values ± SEM (n=3). Statistical analysis was performed by 2-way ANOVA with Bonferroni's post-hoc test, with no significant alteration in response observed.